Predicting forest fires burned area and rate of spread from pre-fire multispectral satellite measurements

Maffei, Carmine; Menenti, Massimo

DOI
10.1016/j.isprsjprs.2019.10.013

Publication date
2019

Document Version
Final published version

Published in
ISPRS Journal of Photogrammetry and Remote Sensing

ISPRS Journal of Photogrammetry and Remote Sensing 158 (2019) 263–278

Contents lists available at ScienceDirect

ISPRS Journal of Photogrammetry and Remote Sensing

journal homepage: www.elsevier.com/locate/isprsjprs

Predicting forest fires burned area and rate of spread from pre-fire multispectral satellite measurements

Carmine Maffei[a,b,*], Massimo Menenti[c,a]

[a] Faculty of Civil Engineering and Geoscience, Delft University of Technology, Stevinweg 1, 2628CN Delft, the Netherlands
[b] Leicester Innovation Hub, University of Leicester, University Road, LE1 7RH Leicester, UK
[c] State Key Laboratory of Remote Sensing Science, Institute of Remote Sensing and Digital Earth, Chinese Academy of Sciences, Beijing 100101, China

ARTICLE INFO

Keywords:
MODIS
Perpendicular Moisture Index (PMI)
Fire Weather Index (FWI)
Live fuel moisture content (LFMC)
Conditional probability distribution
Probability of extreme events

ABSTRACT

Operational forest fire danger rating systems rely on the recent evolution of meteorological variables to estimate dead fuel condition. Further combining the latter with meteorological and environmental variables, they predict fire occurrence and spread. In this study we retrieved live fuel condition from MODIS multispectral measurements in the near infrared and shortwave infrared. Next, we combined these retrievals with an extensive dataset on actual forest fires in Campania (13,595 km^2), Italy, to determine how live fuel condition affects the probability distribution functions of fire characteristics. Accordingly, the specific objective of this study was to develop and evaluate a new approach to estimate the probability distribution functions of fire burned area, duration and rate of spread as a function of the Perpendicular Moisture Index (PMI), whose value decreases with decreasing live fuel moisture content (LFMC). To this purpose, available fire data was intersected with MODIS 8-day composited reflectance data so to associate each fire event with the corresponding pre-fire PMI observation. Fires were then grouped in ten decile bins of PMI, and the conditional probability distribution functions of burned area, fire duration and rate of spread were determined in each bin. Distributions of burned area and rate of spread vary across PMI decile bins, while no significant difference was observed for fire duration. Further testing this result with a likelihood ratio test confirmed that PMI is a covariate of burned area and rate of spread, but not of fire duration. We defined an extreme event as a fire whose burned area (respectively rate of spread) exceeds the 95th percentile of the frequency distribution of all observed fire events. The probability distribution functions in the ten decile bins of PMI were combined to obtain a conditional probability distribution function, which was then used to predict the probability of extreme fires, as defined. It was found that the probability of extreme events steadily increases with decreasing PMI. Overall, at the end of the dry season the probability of extreme events is about the double than at the beginning. These results may be used to produce frequently (e.g. daily) updated maps of the probability of extreme events given a PMI map retrieved from e.g. MODIS reflectance data.

1. Introduction

Wildfires are a widespread factor of ecosystem disturbance (Bond et al., 2005), causing invaluable human casualties, negative effects on carbon sequestration and substantial economic loss (FAO, 2007; Montagné-Huck and Brunette, 2018; Pellegrini et al., 2018). Scientific evidence supports the hypothesis that climate change may alter fire dynamics through the direct and indirect effects it exerts on fuel moisture and availability (Pausas and Ribeiro, 2013; Seidl et al., 2017; Williams and Abatzoglou, 2016) and ultimately on the probability distribution of dependent variables such as fire occurrence, burned area and rate of spread (Flannigan et al., 2016; Podschwit et al., 2018; Syphard et al., 2018).

Fire behaviour is determined by a diverse array of static and dynamic factors (Barrett et al., 2016; Faivre et al., 2016; Falk et al., 2007; Lasslop and Kloster, 2017; Littell et al., 2016; Viegas and Viegas, 1994). Among these, weather is an active driver of fuel moisture (Ustin et al., 2009), which in turn affects ignition delay (and thus ease of inception) and flames propagation (Chuvieco et al., 2009; Rothermel, 1972). Indeed, fire danger models rely on meteorological input to process indicators of fuel water content and assess fire behaviour.

The National Fire Danger Rating System used in the United States is a collection of fuel conditions and fire behaviour indicators computed from meteorological measurements, fuel models, climate class and

* Corresponding author at: Faculty of Civil Engineering and Geoscience, Delft University of Technology, Stevinweg 1, 2628CN Delft, the Netherlands.
E-mail addresses: c.maffei@tudelft.nl (C. Maffei), m.menenti@tudelft.nl (M. Menenti).

https://doi.org/10.1016/j.isprsjprs.2019.10.013
Received 7 May 2019; Received in revised form 18 October 2019; Accepted 22 October 2019
Available online 14 November 2019

Nomenclature

BUI	Build Up Index
CLC	CORINE Land Cover
DC	Drought Code
DMC	Duff Moisture Code
EWT	Equivalent Water Thickness
FFMC	Fine Fuel Moisture Code
FWI	Fire Weather Index
GEV	Generalised Extreme Value
GVMI	Global Vegetation Moisture Index
ISI	Initial Spread Index
LFMC	Live Fuel Moisture Content
LST	Land Surface Temperature
NDVI	Normalised Difference Vegetation Index
NDWI	Normalised Difference Water Index
PMI	Perpendicular Moisture Index

slope (Burgan, 1988; Deeming et al., 1977). Fuel condition components are a collection of descriptors of the water content of two classes of live fuels and four classes of dead fuels. The McArthur Forest Fire Danger Index used in Australia works along similar principles, but only contains one drought index related to dead fuels moisture (Griffiths, 1999; Keetch and Byram, 1968; McArthur, 1967). The Canadian Forest Fire Weather Index (FWI) System is based on the progressive processing of meteorological measurements for the production of three dead fuels moisture codes and three fire behaviour indices, and does not include any model of live fuels moisture (Van Wagner, 1987).

The role of live fuels moisture is indeed crucial in predicting fire behaviour, as it can inhibit or promote the spread of fires (Rossa et al., 2016; Rossa and Fernandes, 2017; Ustin et al., 2009). Nevertheless, its value is not adequately represented by fire danger models as it depends, further to the variability of meteorological conditions, also on plant response to it, which is species and landscape specific (Ruffault et al., 2018). This opens to the adoption of Earth observation technologies in fire danger mapping (Leblon, 2005; Stow et al., 2006; Yebra et al., 2018, 2013), as water in leaf tissues affects the radiometric properties of live fuels in a distinguishable way, that can be captured by optical sensors (Bowyer and Danson, 2004; Buitrago Acevedo et al., 2017, 2018; Hunt and Rock, 1989; Mousivand et al., 2014). Pixel-based mapping of fire danger would then be made possible by the wide availability of instruments providing global coverage on a daily basis, such as MODIS on board Terra and Aqua satellites, VIIRS on Suomi NPP and NOAA-20, and SLSTR on Sentinel-3A and -3B.

Several approaches were proposed for the use of remote sensing to evaluate fire danger. A few authors related indirect estimates of plant water stress to fire activity, e.g. through the analysis of time series of optical spectral indices (Bajocco et al., 2015; Burgan et al., 1998; Maselli, 2003), land surface temperature (LST) (Maffei et al., 2018; Menenti et al., 2016), or an integration of both (Jang et al., 2006; Pan et al., 2016). A more direct method is the inversion of radiative transfer models for the estimation of water content in vegetation (Cheng et al., 2014; Verrelst et al., 2015; Zarco-Tejada et al., 2003), but it needs extensive ground measurements to constrain the solutions space (Quan et al., 2015; Riaño et al., 2005; Yebra et al., 2018; Yebra and Chuvieco, 2009). A different approach is the use of spectral indices for the estimation of moisture content, such as the Normalised Difference Water Index (NDWI) (Gao, 1996), the Global Vegetation Moisture Index (GVMI) (Ceccato et al., 2002), and the Perpendicular Moisture Index (PMI) (Maffei and Menenti, 2014).

NDWI and GVMI have been reported in literature as predictors of fire occurrence. NDWI was used along with remotely sensed LST and atmospheric columnar water vapour to predict fire danger (Abdollahi et al., 2018), while time series of this index documented the seasonality of fire occurrence and demonstrated good forecasting capabilities (Huesca et al., 2014, 2009). GVMI was used along with LST, normalised difference vegetation index (NDVI), topography, land cover and human settlements to predict fire occurrence (Pan et al., 2016), although in specific land cover types other spectral indices had a better performance (Cao et al., 2013).

Both NDWI and GVMI were designed to evaluate canopy water content measured as equivalent water thickness (EWT):

$$EWT = (W_f - W_d)/A$$

where W_f is the mass of the fresh leaf, W_d is its corresponding oven dried mass, and A is leaf area. EWT has a direct effect on the optical properties of vegetation, and indeed it is a parameter of leaf radiative transfer models such as PROSPECT (Feret et al., 2008; Jacquemoud and Baret, 1990). The more recently introduced PMI (Maffei and Menenti, 2014) was specifically constructed as sensitive to live fuel moisture content (LFMC). This quantity expresses water content as a percentage of dry leaf mass:

$$LFMC = (W_f - W_d)/W_d \cdot 100$$

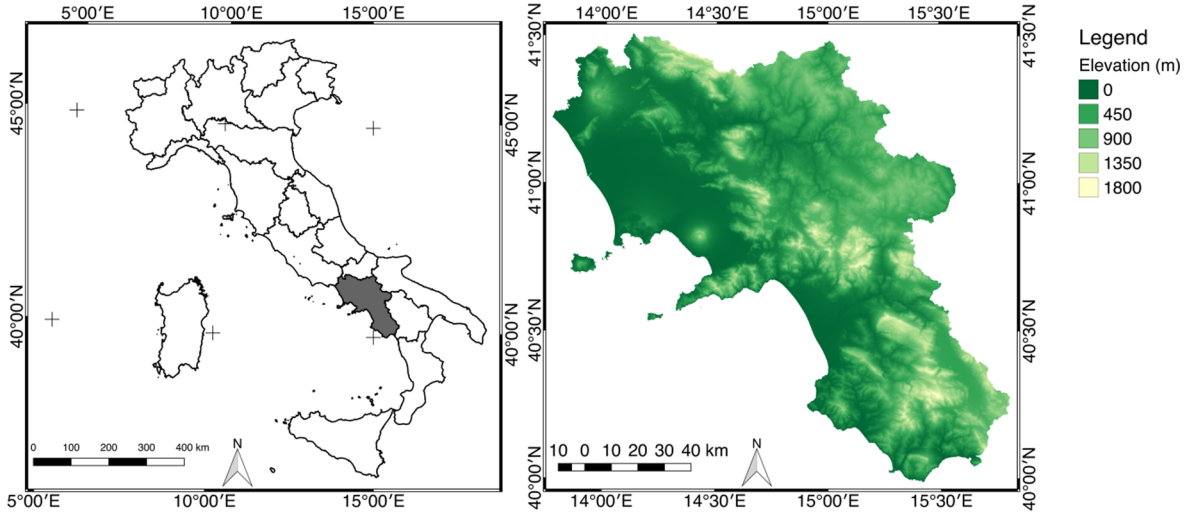

Fig. 1. Study area location map and elevation.

LFMC, along with the corresponding dead fuel moisture content, is a parameter in fire propagation models (Andrews et al., 2013; Finney, 1998; Rothermel, 1991, 1972), and affects probability distribution of burned area and rate of spread (Flannigan et al., 2016; Podschwit et al., 2018). The accuracy of a spectral index in retrieving biophysical quantities is typically assessed against field measurements (Gao et al., 2015; Ullah et al., 2014). However, in the context of the identified need to improve fire danger models through the estimation of LFMC (Ruffault et al., 2018), it would be relevant to investigate the effectiveness of PMI based estimation of LFMC in predicting fire behaviour characteristics that contribute to fire danger such as burned area, duration and spread (Dasgupta et al., 2007), and to evaluate its performance against traditional and trusted fire weather danger rating systems.

The objective of this study was to develop and evaluate a new approach to estimate the probability distribution functions of fire burned area, duration and rate of spread as a function of pre-fire PMI. To this aim, a dataset of ten years of forest fires recorded in the study area of Campania, Italy, was used along PMI maps computed from MODIS reflectance data. The effectiveness of PMI as a covariate of fire behaviour characteristics was then compared against FWI components retrieved from global meteorological reanalysis data. Finally, probability of extreme events conditional to ignition as a function of PMI was evaluated.

2. Materials and methods

2.1. Study area

Campania, Italy (40.83°N, 14.13°E, 13,595 km^2, Fig. 1), is one of the most densely populated and fire affected regions in Mediterranean Europe (Modugno et al., 2016; San-Miguel-Ayanz et al., 2018). Landscape is divided in two main geomorphological areas. Western Campania alternates rocky coasts and alluvial plains. The climate is typically Mediterranean, with average yearly rainfall between 800 and 1000 mm. Summers are hot and dry, while maximum rainfall is recoded in winter. The eastern part of the region comprises mountains and hills. Temperature patterns are determined by altitude, while yearly rainfall reaches 1500 mm, with a maximum in autumn and a minimum in summer (Amato and Valletta, 2017; Fratianni and Acquaotta, 2017). Land cover is dominated by agricultural lands (56% of regional surface) and by forests and semi-natural areas (38%).

2.2. Data

2.2.1. MODIS reflectance data

Satellite reflectance data used in this study is the 8-day composited Aqua-MODIS product (MYD09A1) collection 6 at 500 m resolution (Vermote et al., 1997; Vermote and Vermeulen, 1999). Granules covering months June to September of years 2002–2011 were downloaded from NASA's Land Processes Distributed Active Archive Centre, resulting in a dataset of 163 granules. Retrieved reflectance data were masked against MYD09A1 quality assurance layer, to ensure only the highest quality retrievals are retained. These correspond to band quality assurance bits = 0000 (highest reflectance band quality) and state quality assurance bits 0,1 = 00 (cloud state is clear) (Vermote et al., 2015).

2.2.2. Fire data

The Natural Resources Unit of Carabinieri provided a database of 9127 fires that occurred in Campania between 2002 and 2011. The dataset details for each event, among other information, cartographic coordinates, date and time of initial spread and fire extinction, and final burned area. 913 fires are recorded on average each year, with a mean burned area of 6.2 ha (Table 1). Year 2007 appears to be exceptional in terms of mean burned area (14.7 ha), as this is more than the triple of the mean burned area of all other years (4.2 ha). In this sense year 2011 is representative of baseline mean burned area, although characterised by a high fire occurrence. 99.8% of fires are of anthropic source, either arson or unintentional. The phenomenon peaks in the summer season, with 82% of fires recorded between June and September.

Fires in the dataset were selected for further analyses based on land cover and month of the year. To this purpose, data points were first overlaid over a CORINE Land Cover (CLC) map (European Environment Agency, 2007) to select fires that occurred in natural areas only (Table 2). CLC maps are updated every six years since 2000, so fires were intersected with the closest prior land cover map. Finally, only fires occurring between June and September were selected, leading to a final number of 5005 fires actually retained for subsequent analyses.

This research focussed on burned area, fire duration and rate of spread as fire characteristics potentially related to remote sensing observations of vegetation moisture and meteorological fire danger indices. While burned area is available as a field in the provided database, the latter two variables were computed from available data. Fire duration was evaluated as the difference, in hours, between fire inception and extinction. Rate of spread was calculated from burned area and fire duration in the simplified assumption of a circular fire growing at a constant rate in every direction throughout its duration on a flat and uniform surface.

Burned area, fire duration and rate of spread span over several orders of magnitude, and their distributions appear to be extremely skewed. Prior to any further analysis and to facilitate model fitting, their observations were log-transformed base 10 and shifted, so to have positive values only.

2.2.3. The Canadian Forest Fire Weather Index (FWI) System

The Canadian Forest Fire Weather Index (FWI) System is a collection of six indicators, computed from daily measurements of 24-hour cumulated precipitation, wind speed, relative humidity and air temperature to represent the effect of dead fuels moisture content and of wind on fire behaviour in a standardised fuel type and in no slope conditions (Van Wagner, 1987). It was initially developed to provide a fire danger rating in Canada based solely on weather conditions. Nevertheless, it proved to be a robust mean to effectively map fire danger beyond Canadian climates and biomes (de Groot and Flannigan, 2014; Dowdy et al., 2009; San-Miguel-Ayanz et al., 2012; Taylor and Alexander, 2006).

In detail, the FWI system is composed of: Fine Fuel Moisture Code (FFMC), Duff Moisture Code (DMC) and Drought Code (DC), which are representative of the moisture content of three different classes of dead fuels; Initial Spread Index (ISI), providing a measure of rate of spread, independently of the variable quantity of fuels; Build-Up Index (BUI), a descriptor of the fuels available for combustion; Fire Weather Index (FWI), a comprehensive indicator related to fire intensity.

These indicators develop over different ranges of values, and danger thresholds are usually identified locally based on fire history (Van Wagner, 1987). Each component of the FWI system carries a different layer of information on fire danger. FFMC provides a measure of ease of

Table 1
Summary statistics of forest fires in the study area.

Year	Number of fires	Mean burned area (ha)	Proportion of fires exceeding 95th percentile of burned area
2002	310	3.8	1.9%
2003	1323	4.1	2.3%
2004	803	3.9	2.5%
2005	669	2.9	1.2%
2006	423	4.1	3.5%
2007	1757	14.7	13.4%
2008	776	4.4	3.6%
2009	895	5.8	5.6%
2010	537	3.7	1.9%
2011	1634	4.2	3.0%

Table 2
CORINE Land Cover (CLC) classes associated with fires for subsequent analyses.

CLC code	Description
231	Pastures
243	Land principally occupied by agriculture, with significant areas of natural vegetation
311	Broad-leaved forest
312	Coniferous forest
313	Mixed forest
321	Natural grassland
323	Sclerophyllous vegetation
324	Transitional woodland shrub
333	Sparsely vegetated areas
334	Burnt areas

fire inception and flammability of the top fuel layer, where initial ignition usually occurs. DMC and DC are rather related to fuel consumption of medium and large sized woody material. ISI is generally related to burned area, as it combines fine fuel moisture content and wind speed, both relevant to this fire characteristic. BUI is a good predictor of fire behaviour and fuel consumption. FWI, as a synthesis of the other five indices, is generally related to several descriptors of fire activity.

In this research, FWI layers were retrieved from the Global Fire Weather Database (Field et al., 2015). These layers are computed from NASA Modern Era Retrospective Analysis for Research and Applications version 2 global meteorological reanalyses of air temperature, relative humidity, wind speed and precipitation (Molod et al., 2015), and distributed at a resolution of 0.25° × 0.25° (about 21 × 28 km^2 at the latitude of the study area).

2.3. The Perpendicular Moisture Index

The Perpendicular Moisture Index (PMI) was developed from the observation that in a plane reporting MODIS reflectance at 0.86 μm (channel 2) and 1.24 μm (channel 5), isolines of LFMC are straight and parallel (Maffei and Menenti, 2014). The PMI is thus evaluated as the distance of reflectance points from a reference line:

$$PMI = -0.73 \cdot (R_{1.24\mu m} - 0.94 \cdot R_{0.86\mu m} - 0.028)$$

In this sense, PMI is a direct measure of LFMC, with higher values corresponding to higher moisture content.

2.4. Parametric distributions of fire characteristics

To evaluate the distribution of fire characteristics conditional to PMI and FWI components, parametric distributions describing burned area, fire duration and rate of spread in the study area were first identified. Tested distributions were selected from existing literature (Baker, 1989; Corral et al., 2008; Cumming, 2001; Haydon et al., 2000; Moritz, 1997; Reed and McKelvey, 2002; Weber and Stocks, 1998), and included normal, log-normal, exponential, gamma, generalised extreme value (GEV) and Weibull. Available fire data were fitted to the named distribution through the minimisation of the Anderson-Darling distance (Anderson and Darling, 1954), and the closest fitting model for each fire characteristic was retained as a basis for further analyses (Hernandez et al., 2015; Maffei et al., 2018).

2.5. Conditional distributions of fire characteristics

PMI maps were produced from available MYD09A1 data and sampled at fire locations on the compositing period prior to the event.

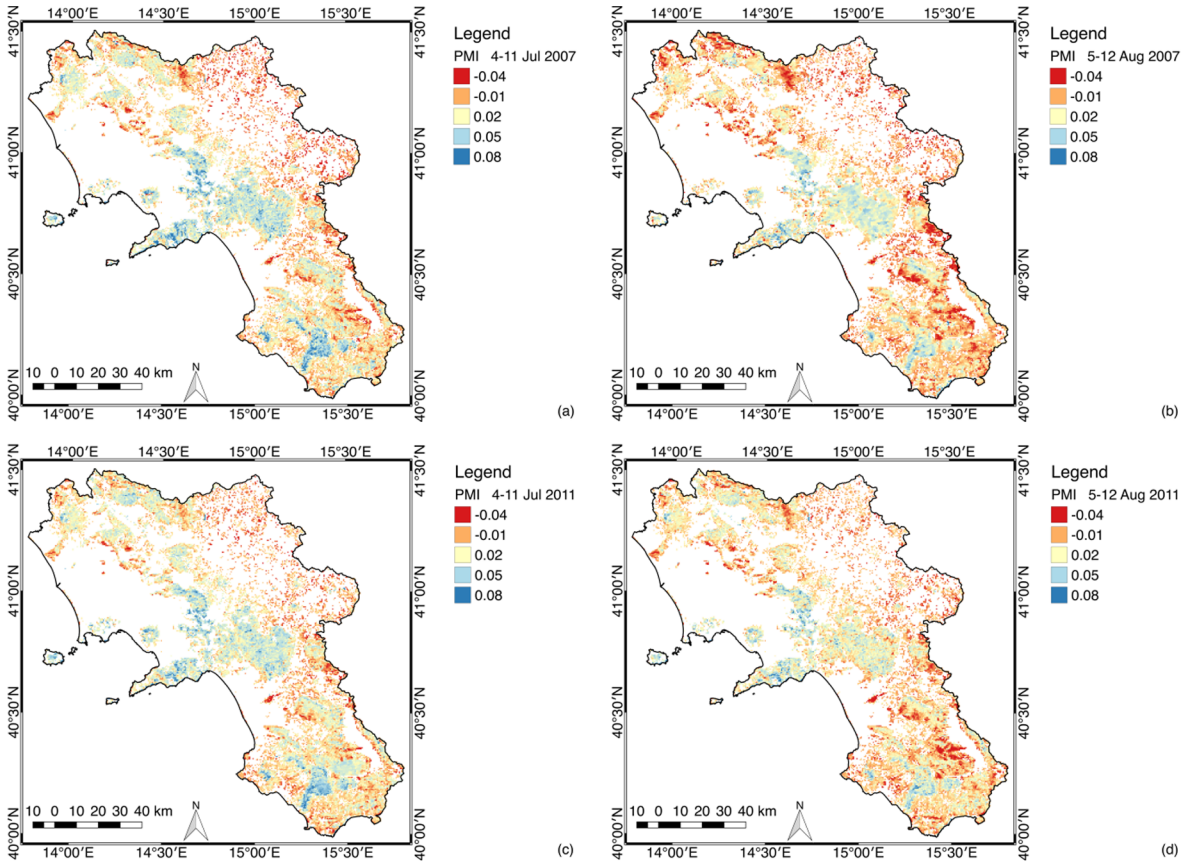

Fig. 2. Selected PMI maps derived from Aqua-MODIS 8-day reflectance composites showing intra- and inter-annual variability: 4–11 July 2007 (a), 5–12 August 2007 (b), 4–11 July 2011 (c), 5–12 August 2011 (d).

Similarly, maps of the six FWI components were sampled on the day of the event. This resulted in each fire in the database being associated with the corresponding PMI recorded in the raster cell where it occurred in the antecedent 8-day MODIS compositing period as well with the corresponding daily value of the six FWI components in the respective raster cell.

To understand whether PMI and the six FWI components may be considered a covariate of fire characteristics, their observations were divided in ten decile bins. The parameters of the corresponding distributions were then retrieved in each bin with the Anderson-Darling maximum goodness of fit criterion, and their 95% confidence intervals were determined by means of 1000 bootstrap estimations (Hernandez et al., 2015; Maffei et al., 2018).

To assess the significance of observed distribution parameters across the decile bins, a likelihood ratio test was performed comparing, for PMI and for each of the FWI components, the sum of the likelihoods of the ten models fitted in the individual bins (alternative models) to the likelihood of the unconditional model fitting all log-transformed burned area, fire duration and rate of spread data (null models). Test significance was set at 0.05.

2.6. Conditional probability of extreme events

The identified conditional probability distribution functions were further used to evaluate the probability of extreme events conditional to ignition as a function of PMI. Probabilities were computed by modelling the dependence of the corresponding distribution parameters on PMI. For the purpose of this study, an event was considered extreme if it exceeded the 95th percentile of burned area, fire duration and rate of spread values observed in the study area. The 95th percentile of burned area of summer fires in natural areas is 30.0 ha, of fire duration is 28.2 h, of rate of spread is 48.4 m/h.

3. Results

3.1. Temporal and spatial variability of PMI

Maps of PMI exhibit significant inter- and intra-annual variability, as for example the four PMI maps representing compositing periods 4–11 July and 5–12 August of years 2007 and 2011 (Fig. 2). Spatial patterns of PMI in the 5–12 August period show lower values as compared to 4–11 July in both years, corresponding to lower LFMC. Moreover, both compositing periods show in 2007 lower values than the corresponding periods in 2011.

To synthetically visualise seasonal evolution, median PMI was computed in each of the selected land cover classes (Table 2) across the dry season of years 2002–2011. While maps are characterised by a continuity of values, discretised in raster cells, this synthesis approach has the advantage of highlighting differences across land cover classes in observed PMI (and indirectly LFMC) values. A consistent reduction of PMI, corresponding to a reduction in LFMC, is observed throughout the dry season for all classes in all years, as for example in 2007 and 2011 (Fig. 3). The dynamic of such reduction shows inter-annual variability, as it can be here noticed with the higher medians (higher LFMC) recorded in 2011.

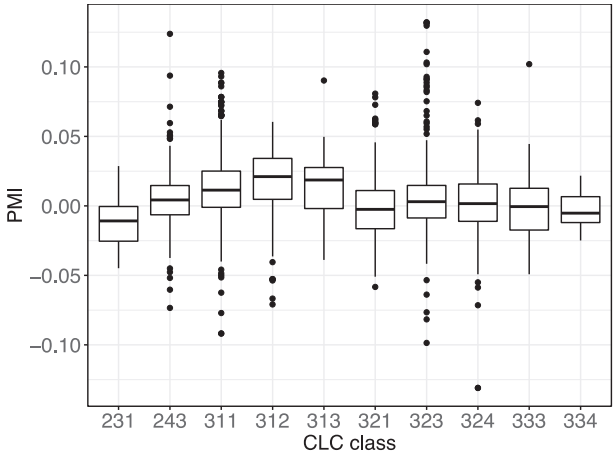

Fig. 4. Boxplot of PMI observed at fire location in each CLC class (Table 2).

The observed diverse median values recorded in each CLC class are reflected in the PMI values recorded at fire locations (Fig. 4). Indeed, lower PMI observations (and thus lower LFMC) are recorded at fires occurring in pastures and sparsely vegetated areas. Conversely, fires tend to be recorded with higher PMI values (higher LFMC) in broad leaved, coniferous and mixed forests.

3.2. Probability models of fire characteristics

Log-transformed burned area, fire duration and rate of spread were fitted to normal, log-normal, exponential, gamma, GEV and Weibull distributions, and the corresponding Anderson-Darling statistics are reported in Table 3. Normal is the closest fitting distribution of log-transformed burned area, while GEV is the closest model for log-transformed fire duration and Weibull for log-transformed rate of spread. The corresponding Q-Q plots are reported in Fig. 5.

3.3. Conditional distributions of fire characteristics

The mean of the normal distribution of log-transformed burned area conditional to PMI in ten decile bins shows a significant ($p < 0.001$)

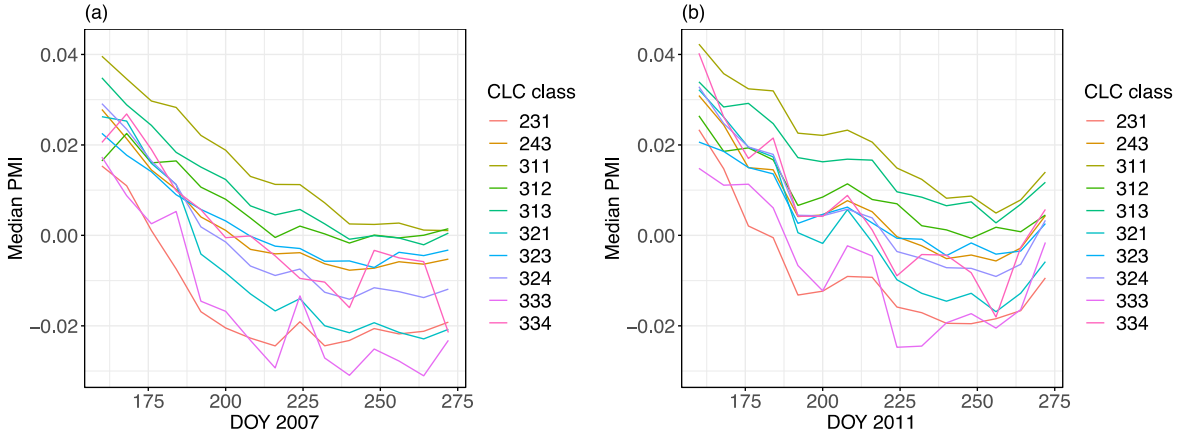

Fig. 3. Evolution of the median PMI value in CLC classes (Table 2) during the dry season in two selected years: 2007 (a), 2011 (b).

Table 3
Anderson-darling statistic values for tested distributions. Lower values indicate a closer fit.

Model	Log-transformed burned area	Log-transformed fire duration	Log-transformed rate of spread
Normal	7.2	52.3	20.3
Log-normal	16.7	20.4	40.8
Exponential	1347	1387	1559
Gamma	11.0	28.7	33.1
Generalised Extreme Value (GEV)	10.5	10.5	39.6
Weibull	25.2	134	8.2

decreasing ($r^2 = 0.80$) trend with increasing PMI (Fig. 6a). The variation of standard deviation appears non-significant when evaluated against a linear model, and the confidence intervals of this parameter are consistent with a constant value across most PMI bins (Fig. 6b). For log-transformed fire duration, no significant trend was observed in location and shape of GEV distribution conditional to PMI, and a weak increasing trend ($r^2 = 0.53$, $p < 0.05$) in scale (Fig. 7). Both parameters of the Weibull distribution of log-transformed rate of spread show significant ($p < 0.001$) decreasing trends ($r^2 = 0.84$ and $r^2 = 0.96$ respectively) with increasing PMI (Fig. 8). These observations support the idea that PMI is a covariate of burned area and rate of spread, while its contribution to fire duration probability distribution is weak or not significant.

The variability of the parameters of the normal distribution of burned area in ten decile bins of FWI components support the idea that all six components are a covariate of burned area (Fig. 9). Mean increases linearly with all components with $p < 0.001$ and r^2 ranging between 0.84 and 0.96, substantially covering the same range of values covered against PMI. A significant linear variation of the standard deviation is observed only with DMC and BUI ($p < 0.001$ and $p < 0.01$ respectively). Similar observations can be drawn for fire duration, with location, scale and shape of GEV distribution varying linearly with the respective FWI components with significance at least $p < 0.001$ for location and at least $p < 0.05$ for scale and shape (Fig. 10). The contribution of FWI components to the variability of the Weibull distribution of log-transformed rate of spread is less evident as compared against the other fire characteristics (Fig. 11). Shape shows significant trends only conditional to DMC ($r^2 = 0.50$, $p < 0.05$), DC ($r^2 = 0.66$, $p < 0.01$) and BUI ($r^2 = 0.46$, $p < 0.05$), while scale shows significant trends only conditional to DC ($r^2 = 0.59$, $p < 0.01$) and BUI ($r^2 = 0.67$, $p < 0.01$). Moreover, the observed trends show limited sensitivity as compared to PMI (Fig. 8).

The likelihood ratio test (Table 4) confirms that all models conditional to PMI and to the six FWI components (alternative models) allow the rejection of the null model fitting all log-transformed burned area data. Among the alternative models, PMI ensures the highest summed likelihood. The test confirms that the alternative fire duration model conditional to PMI fails to reject the null model, while DMC shows the highest summed likelihood among the FWI components. FFMC, DMC and DC fail to reject the null model of rate of spread, while PMI ensures the alternative model with the highest likelihood. These results confirm PMI is a covariate of burned area and rate of spread, but not of fire duration.

3.4. Conditional probability of extreme events

From the observations above, a linear relationship was adopted to model the dependence of the mean of the normal distribution of log-transformed burned area on PMI, while for the standard deviation the constant value of the general model was adopted (Fig. 6). For log-transformed rate of spread, a linear model was adopted for both the shape and the scale of the Weibull distribution (Fig. 8). The resulting conditional probabilities over a range of PMI values are plotted in Fig. 12. With decreasing PMI (and thus decreasing LFMC) the probability of a fire larger than 30 ha conditional to ignition increases from 1.8% to 7.4%. Similarly, the probability of a rate of spread higher than 48.4 m/h conditional to ignition raises from 1.2% to 10.5%.

4. Discussion

This study had the stated objective of developing and evaluating a new approach to estimate the probability distribution functions of fire behaviour characteristics as a function of PMI. Those investigated herein, as allowed by the available fire data, included rate of spread, burned area and duration. With climate change altering weather patterns worldwide, and ultimately affecting fire regimes (Seidl et al., 2017), there is an increasing need to improve fire danger rating models and use synergistically the information they deliver (Chowdhury and Hassan, 2015; Ruffault et al., 2018; Yebra et al., 2013). To support their preparedness activities, fire managers are interested in predicting fire occurrence and behaviour. Our approach, as based on probabilities of event properties rather than on their deterministic modelling, suits the need to predict fire danger.

Precondition for fire occurrence is the ease of ignition, which is determined by dead fuel moisture content (Aguado et al., 2007; Bianchi and Defossé, 2014; de Groot et al., 2005). Operational fire danger rating systems estimate this parameter from meteorological measurements (Burgan, 1988; Deeming et al., 1977; Keetch and Byram, 1968; McArthur, 1967; Van Wagner, 1987). Fire behaviour depends on a diverse array of factors, among which the moisture content of both dead and live fuels plays a significant role as it directly affects flame propagation (Rothermel, 1972). Vegetation moisture content is determined by plant active response to weather conditions as regulated by transpiration, and by dry mass changes associated with phenology, both processes being species specific. For this reason, the simplified approach for the estimation of LFMC in fire danger models results in lack

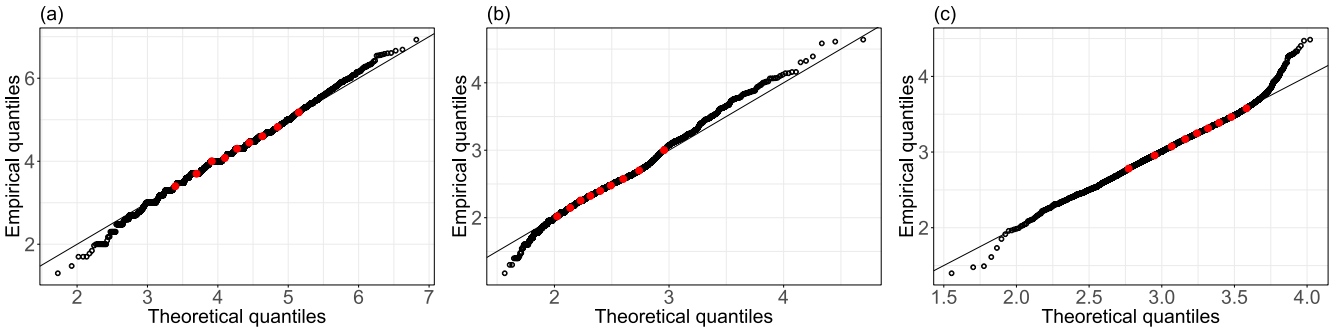

Fig. 5. Q-Q plots of the normal distribution of log-transformed burned area (a), of the GEV distribution of log-transformed fire duration (b) and of the Weibull distribution of log-transformed rate of spread (c). Red circles indicate the deciles of the distributions.

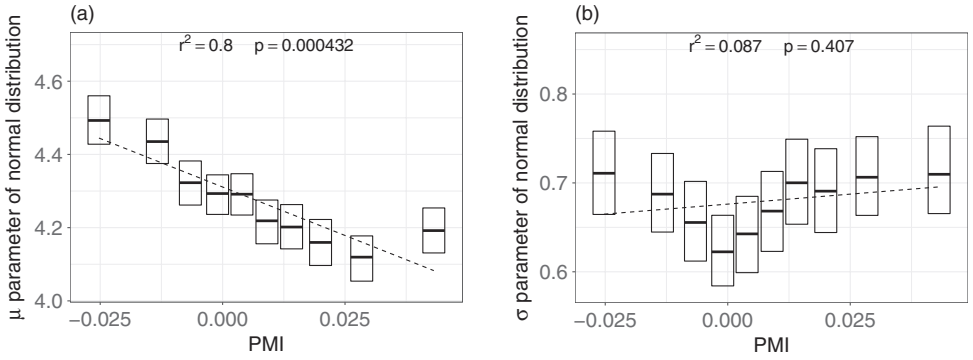

Fig. 6. Plots of mean (a) and standard deviation (b) of normal distribution of log-transformed burned area, and their 95% confidence intervals, in ten decile bins of PMI. Regression lines refer to the estimated parameters.

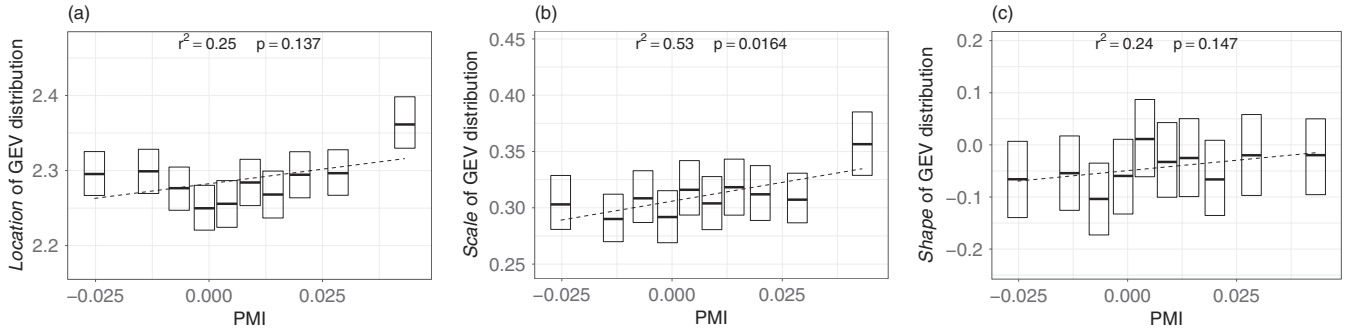

Fig. 7. Plots of location (a), scale (b) and shape (c) of GEV distribution of log-transformed fire duration, and their 95% confidence intervals, in ten decile bins of PMI. Regression lines refer to the estimated parameters.

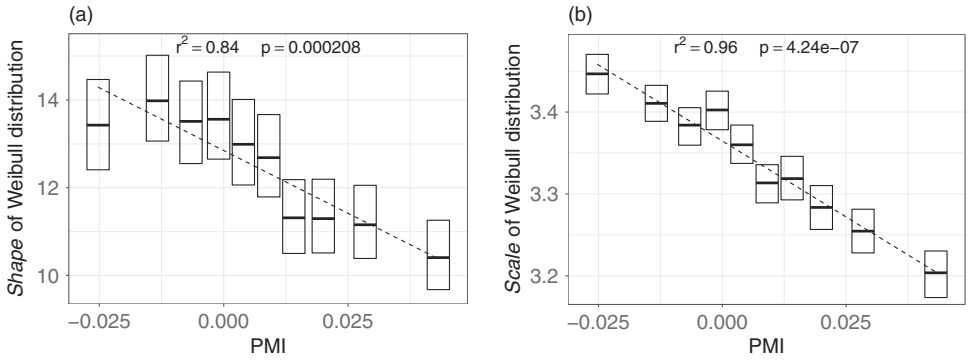

Fig. 8. Plots of shape (a) and scale (b) of Weibull distribution of log-transformed rate of spread, and their 95% confidence intervals, in ten decile bins of PMI. Regression lines refer to the estimated parameters.

of generality (Jolly and Johnson, 2018; Nolan et al., 2018; Pellizzaro et al., 2007b; Ruffault et al., 2018).

In this research we use the Perpendicular Moisture Index (PMI) as an indicator of LFMC. Indeed, remote sensing measurements in the near infrared and in the shortwave infrared allow for the quantification of water content in leaf tissues (Gates et al., 1965; Gausman and Allen, 1973; Tucker, 1980; Woolley, 1971). Among the various broadband spectral indices of vegetation moisture, the focus on the PMI is motivated by its initial development with respect to general spectral index development methods (Ceccato et al., 2002; Dasgupta and Qu, 2009; Huete, 1988; Verstraete and Pinty, 1996) maximising its sensitivity to LFMC variations (Maffei and Menenti, 2014). This feature allows for its use along with existing fire danger models. Our approach is opposed to that of the Wildland Fire Assessment System services of the US Forest Service, which is based on the processing of time series of the NDVI for the evaluation of relative greenness (Preisler et al., 2009). Indeed, the Fire Potential Index produced by the Wildland Fire Assessment System is a predictor of fire occurrence, and is not integrated in fire behaviour components of the National Fire Danger Rating System (Chowdhury and Hassan, 2015).

The analyses were conducted in the study area of Campania (13,595 km^2), an Italian region characterised by the diversity of its landscape and listed as one of the most fire prone in the Mediterranean. Fire data was provided by Carabinieri, a law enforcement agency, and as such it can be considered official and correct. Provided data points correspond to the centroid of the burned area, but the exact burnt scar perimeters were not part of the dataset. While in general this might arise concerns around positional accuracy of the available coordinates against gridded MODIS reflectance composites, it must be observed that fire regime is dominated by a large number of small fires, and indeed only 4.5% of fires in the database resulted in a burned area larger of a 500 × 500 m^2 MODIS pixel, and 0.7% larger than 1 km^2. This means that positional accuracy of fire data is substantially of the same order of magnitude of positional accuracy of MODIS data (Wolfe et al., 2002).

Adding to this, as a consequence of the coarse MODIS resolution, the PMI value associated with each fire does not correspond to the PMI value of the specific vegetation patch where fire was ignited. This is not relevant for the purpose of this study, as the retrieved PMI was hereby regarded as a measure of the environmental conditions in the cell including the centroid of the burned area (Pyne et al., 1996). This is consistent with our use of PMI values to estimate the parameters of the probability distribution functions of fire characteristics applying to a cell, rather than for the construction of deterministic models linking satellite observations of LFMC to burned area and rate of advancement of flames.

For its nature, the fires dataset does not contain information on fire behaviour. However, it reports burned area and duration, while rate of spread was computed from these factors under the simplified assumption of a circular fire growing at a constant rate in every direction throughout its duration on a flat and uniform surface. Rate of spread is generally defined as "the relative activity of a fire in extending its horizontal dimensions", and the way it is expressed depends on the intended use of this information (FAO, 1986). As used in this research, rate of spread is the rate of advancement of fire perimeter, in metres per hour. While this quantity does not directly relate to the local rate of advancement of flames, it is a measure of the average growth rate of a

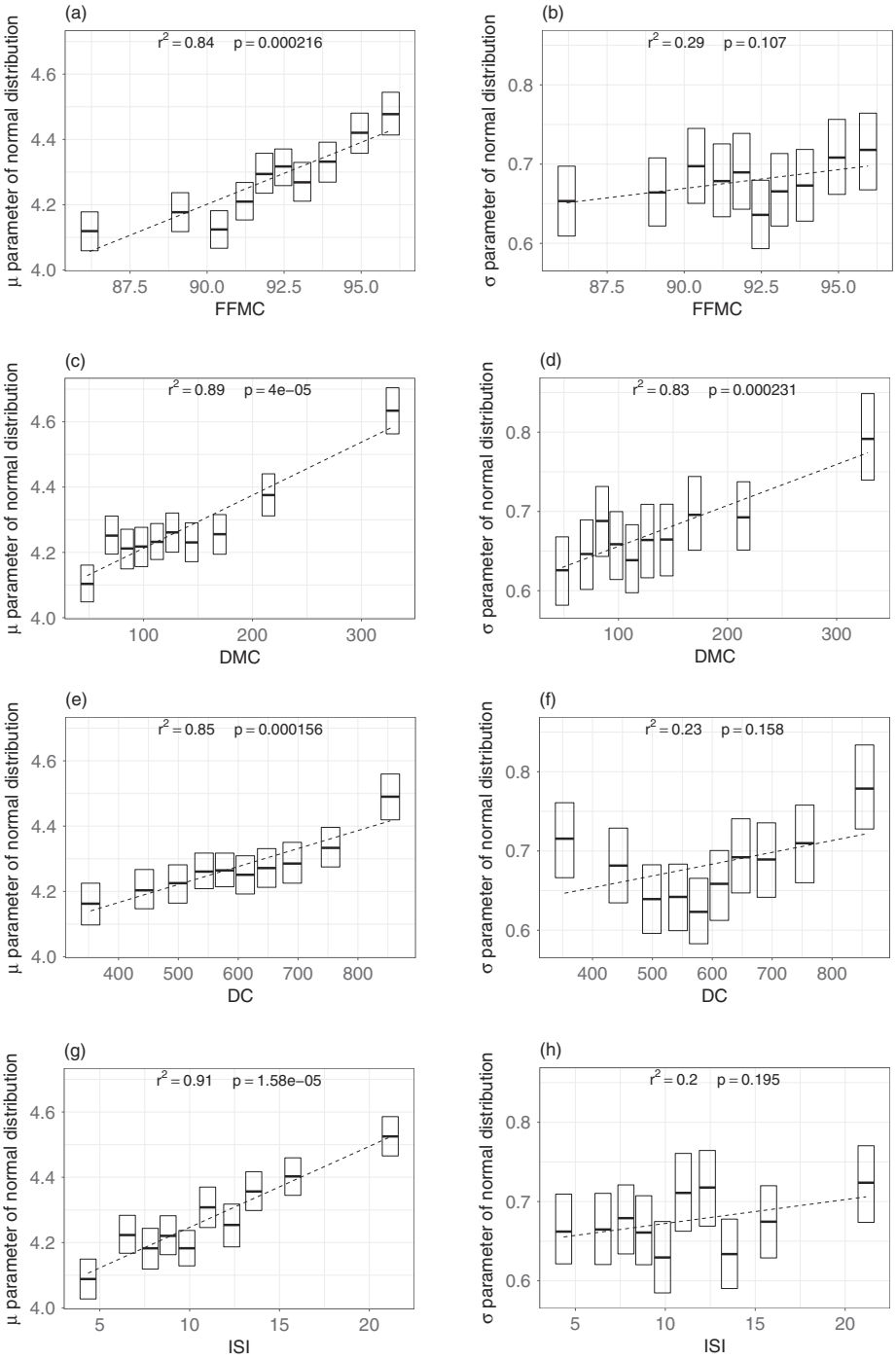

Fig. 9. Plots of mean and standard deviation of normal distribution of log-transformed burned area, and their 95% confidence intervals, in ten decide bins of the Canadian Forest Fire Weather Index System components: FFMC (a, b), DMC (c, d), DC (e, f), ISI (g, h), BUI (i, j), FWI (k, l). Regression lines refer to the estimated parameters.

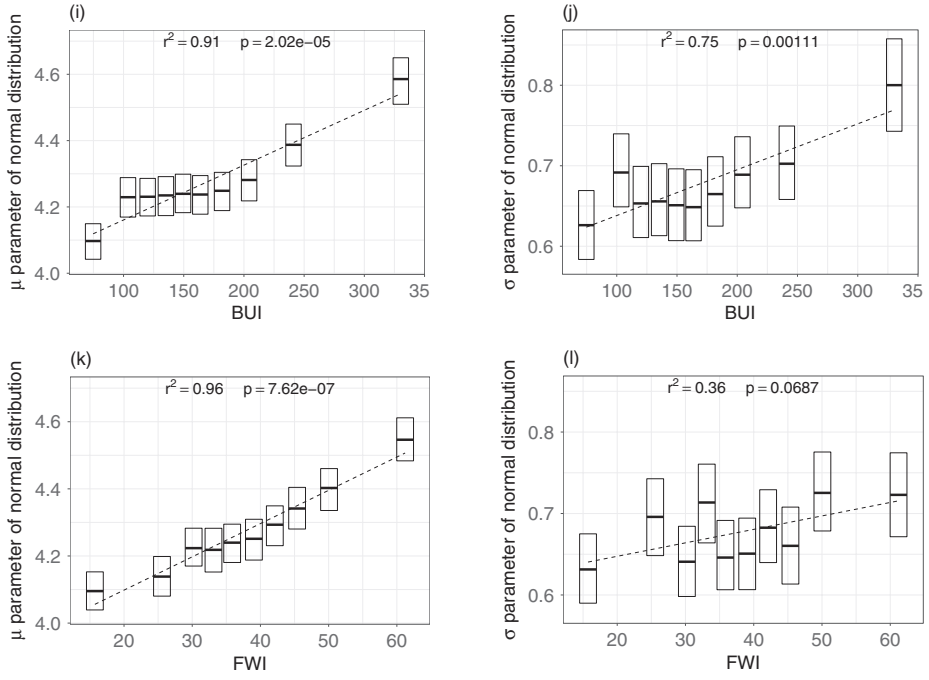

Fig. 9. (*continued*)

fire, and indirectly of the difficulty to control it. In fact, fire danger models are aimed at segmenting landscape in fire danger classes and not at modelling the propagation of flames.

Fires in the database were associated with the PMI values recorded in the pre-fire 8-day MODIS compositing period. The choice of sampling PMI from the antecedent compositing period was dictated by the need to ensure reflectance data is not contaminated by burnt scar, while simulating a typical operational scenario where this MODIS product would be used in the period building towards the availability of the following composite. The length of the compositing period and the use of the pre-fire composited granule do not pose a problem with regards to variations in LFMC. Indeed, vegetation moisture is not subject to abrupt changes over short periods of time (Leblon et al., 2001; Vicente-Serrano et al., 2013). With operational scenarios in mind, FWI maps were sampled on the day of the event, as this type of product is typically available on a daily basis and produced from weather forecasts.

Spatial patterns of PMI show clear seasonal and interannual variability, as for the example shown in Fig. 2. Moreover, the temporal evolution of the median PMI per land cover class shows a steady decreasing trend throughout the dry season in each observation year, although at a different rate, with Fig. 3 reporting the examples of years 2007 and 2011. This observation corresponds to a reduction of LFMC throughout the dry season, and is in line with findings on the seasonal evolution of LFMC in Mediterranean ecosystems (Pellizzaro et al., 2007a, 2007b; Ruffault et al., 2018). The increase in PMI, and thus in LFMC, observed in September 2011 is likely due to abundant rainfall registered in the region (data from http://agricoltura.regione.campania.it/meteo/agrometeo.htm, last accessed 17th October 2019).

Fire events are recorded at PMI values that appear to depend on land cover classes (Fig. 4). The highest PMI values, corresponding to higher LFMC, are observed in coniferous forests whereas the lowest values are observed in pastures. This result was expected (Barrett et al., 2016; Faivre et al., 2014) and it is due to the varying effect of species composition and structure on their flammability (Dimitrakopoulos, 2001; Dimitrakopoulos and Panov, 2001; Dimitrakopoulos and Papaioannou, 2001).

This study is based on the initial identification of the probability distribution functions fitting available data on burned area, fire duration and rate of spread (Hernandez et al., 2015; Maffei et al., 2018). Several probability models fitting fire data are reported in literature (Baker, 1989; Corral et al., 2008; Cumming, 2001; Haydon et al., 2000; Moritz, 1997; Reed and McKelvey, 2002; Weber and Stocks, 1998). Indeed, fire behaviour is determined by a wide array of factors, most of which are related to the specific physical and environmental conditions of the area under investigation. This suggested the ad hoc identification of the probability distributions that best adapted to describe fire characteristics as shaped by the unique combination of landscape and environmental factors in Campania (Cui and Perera, 2008; Reed and McKelvey, 2002). It was found that log-transformed burned area is described by a normal distribution, log-transformed fire duration by a GEV distribution, and log-transformed rate of spread by a Weibull distribution.

The mean of the normal distribution of log-transformed burned area conditional to PMI shows a significant decreasing linear trend, whereas the standard deviation can be safely be assumed to be constant (Fig. 6). This would be expected, as a lower moisture content leads to a quicker propagation of flames and ultimately to a larger burned area (Rothermel, 1972). Likelihood ratio test (Table 4) confirms that the summed likelihood of the ten models constructed in decile bins of PMI (alternative model) allows the rejection with significance 0.05 of the null model where PMI is not a covariate of burned area. In other terms, the alternative model is a better probability model for observed burned area. Overall, these findings confirm that PMI is a covariate of burned area. Rate of spread shows similar results, with both parameters of the Weibull distribution conditional to PMI reporting decreasing trends (Fig. 8) and the likelihood ratio test confirming rejection of the unconditional model (Table 4).

Scale is the only parameters of the GEV distribution of log-transformed fire duration exhibiting a significant trend across the ten decile bins of PMI, yet over a limited range of values (Fig. 7). Indeed, confidence intervals of this parameter are consistent with a constant value across most PMI bins. In fact, the alternative (conditional) model fails to reject the null model (Table 4), and PMI can't be considered a covariate of fire duration.

These comments support the potential role of remote sensing measurements in contributing to fire danger mapping, as probability distributions of burned area and rate of spread are clearly affected by PMI variability. This is the same effect that would be expected from the

variability of fuel moisture content (Flannigan et al., 2016; Podschwit et al., 2018; Syphard et al., 2018). This potential was further assessed through comparison with FWI. The reanalysis data adopted herein has a resolution of 0.25° × 0.25° (about 21 × 28 km^2 at the latitude of the study area), while operational services are available at a resolution of 10 km (San-Miguel-Ayanz et al., 2018). This results in a substantial lack of detail, as opposed to MODIS reflectance data available at 500 m resolution. However, resolution of FWI data used herein is still capable of capturing broad weather differences typically occurring in the study area, especially across its geomorphologic and climatic East-West gradient (Amato and Valletta, 2017; Fratianni and Acquaotta, 2017).

The mean of the normal distribution of log-transformed burned area conditional to the six FWI components increases with all of them, while standard deviation can be assumed constant, as justified by most confidence intervals for all indices (Fig. 9). All FWI components were designed on individual scales, but with the clear meaning of higher values corresponding to higher danger. This finding implies that at increasing danger values the mean burned area of occurred fires was higher. The closer fit with fire behaviour indices can be explained by the fact that ISI, BUI and ultimately FWI combine information from drought indices and weather inputs, and thus tend to be better indicators of several aspect of fire activity (Van Wagner, 1987).

A similar observation can be drawn for log-transformed fire duration (Fig. 10), where the variability of the parameters of the GEV distribution conditional to FWI components justify increasing probability of longer fire duration with increasing danger, and where BUI and FWI show the closest fits. This is reflected in the corresponding likelihood ratio tests, with all conditional distributions (alternative models)

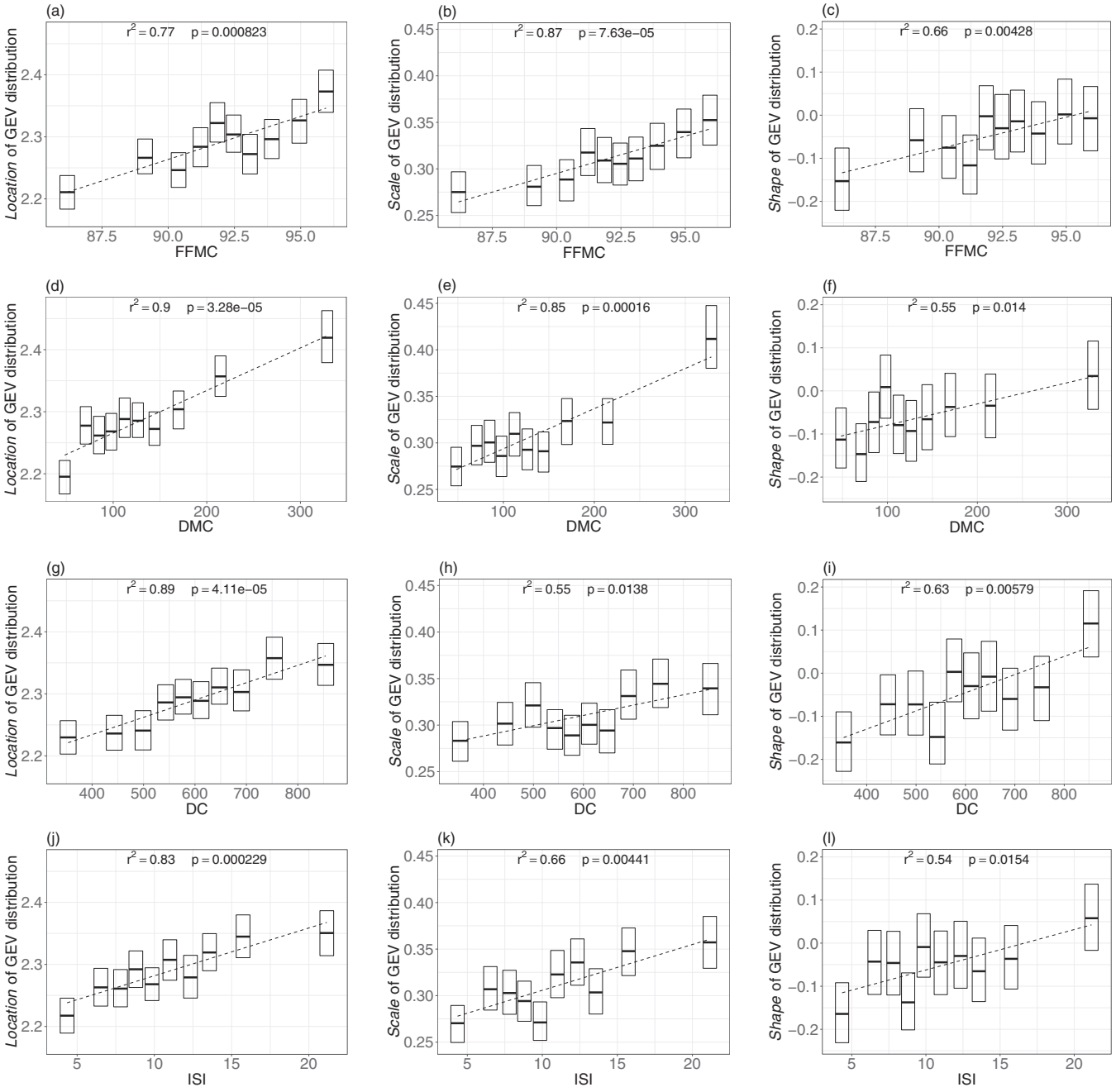

Fig. 10. Plots of location, scale and shape of GEV distribution of log-transformed fire duration, and their 95% confidence intervals, in ten decide bins of the Canadian Forest Fire Weather Index System components: FFMC (a, b, c), DMC (d, e, f), DC (g, h, i), ISI (j, k, l), BUI (m, n, o), FWI (p, q, r). Regression lines refer to the estimated parameters.

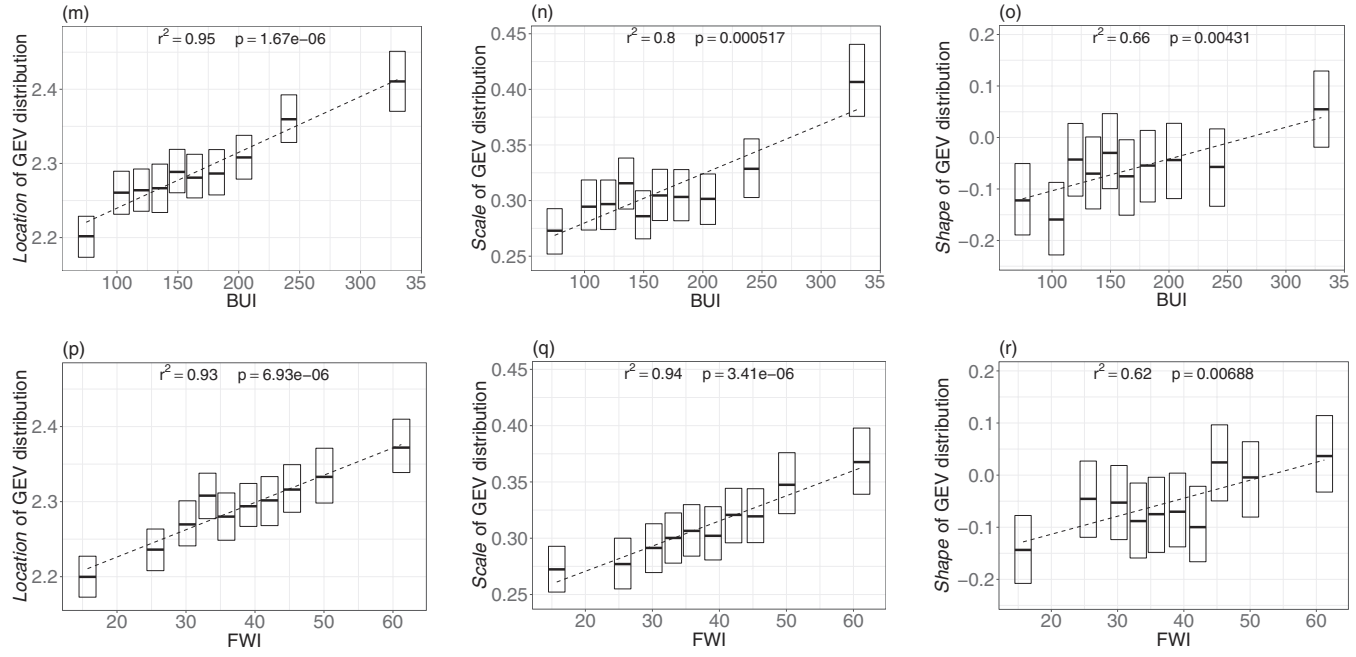

Fig. 10. (*continued*)

Table 4
Results of the likelihood ratio test. Null model is the one fitting all data. Alternative model is the collection of ten models in decile bins of the candidate covariate. Significance level is 0.05. In bold the alternative models showing the highest likelihood for each fire characteristic.

	Burned area	Duration	Rate of spread
PMI	**Rejection**	Non-rejection	**Rejection**
FFMC	Rejection	Rejection	Non-rejection
DMC	Rejection	**Rejection**	Non-rejection
DC	Rejection	Rejection	Non-rejection
ISI	Rejection	Rejection	Rejection
BUI	Rejection	Rejection	Rejection
FWI	Rejection	Rejection	Rejection

rejecting the null model, and the FWI components showing to be a covariate of fire duration where PMI is not (Table 4).

The relationship between FWI components and the parameters of the Weibull distribution of log-transformed rate of spread shows some ambiguities, with no trends against FFMC, ISI and FWI, and slightly decreasing trends against DMC, DC and BUI (Fig. 11). The latter result is counterintuitive, as is corresponds to a substantial decrease in rate of spread with increasing fire danger. Moreover, it contrasts with findings against PMI, where rate of spread increases with decreasing PMI (Fig. 6). In fact, BUI is an indicator of fire activity and its value, along with its contributing factors DMC and DC, slowly increases throughout the dry season. This means that other seasonal dependent factors relevant to rate of spread, such as winds, might be having a predominant effect with BUI and the two moisture codes here acting as a proxy for them (Van Wagner, 1987).

The likelihood ratio tests on the probability models of rate of spread show that the alternative models conditional to FFMC, DMC and DC fail to reject the null model, as opposed to those conditional to ISI, BUI and FWI (Table 4). The most problematic are the alternative models conditional to ISI and FWI, which allow the rejection of the corresponding null models although conditional model parameters do not exhibit any significant trend. The result of the likelihood ratio test may be explained by an overfitting caused by the wide variability observed in the values of the conditional shape across the bins (Fig. 11 g and k). Indeed, rejection of the null model does not directly imply that the alternative model is to be preferred. On the other side, the alternative model conditional to DC fails to reject null model, despite the significant trends observed in both shape and scale (Fig. 11 e and f). In this case, it can be observed that a constant value fits most of the confidence intervals in both parameters. The latter comment also applies to BUI (Fig. 11 i and j), although the corresponding alternative model allows for the rejection of the null model. Overall, these notes contrast with the net trend of parameters conditional to PMI and to their narrower confidence intervals (Fig. 8). In fact, the alternative model conditional to PMI shows a likelihood higher than any FWI component (Table 4).

These results allow the computation of actionable information (Preisler et al., 2004) in the form of probability of extreme events conditional to ignition as a function of PMI (Fig. 12). Clearly, forest fires in the study area are relatively small as compared to other areas worldwide. Yet defining as extreme events those that are above the 95th percentile in terms of burned area or rate of spread is appropriate in this specific context, as it refers to the most demanding events the local authorities are faced with in terms of deployed resources for their containment in a highly anthropized and fragmented landscape. Bearing in mind that several other factors contribute to fire behaviour, and thus to the probability distribution functions of burned area and rate of spread, it is here observed an increasing probability of extreme events conditional to ignition with a reduction in PMI, and thus in LFMC. This is in line with expectations, and indirectly confirms the role of LFMC in driving fire behaviour (Nolan et al., 2016; Pimont et al., 2019; Ruffault et al., 2018). When compared against the observed evolution of median PMI across the fire season (Fig. 3), the probability of extreme events at the end of the fire season is about the double than at the beginning.

5. Conclusions

This study demonstrated that satellite observations of LFMC by means of the PMI contribute to the prediction of the probability distributions of forest fires burned area and rate of spread, and that probability distribution functions conditional to PMI describe observations with a higher likelihood than the unconditional models. In other terms, it was demonstrated that PMI is a covariate of both burned area and rate of spread. Remote sensing measurements in the solar spectrum are thus a viable mean to complement existing fire danger

mapping tools, contributing to the prediction of the probability of extreme events conditional to ignition.

Analyses described herein were performed on MODIS data. However, any sensor collecting measurements in the near infrared and shortwave infrared can be used to compute the PMI. Adding to MODIS, daily global observations are available from the two pairs of VIIRS and SLSTR sensors. This enables the daily availability of PMI maps at a resolution that is one order of magnitude higher than existing operational fire danger services based on meteorological data (Burgan, 1988; San-Miguel-Ayanz et al., 2012). Similar bands are also available in higher resolution sensors such as OLI on board Landsat 8 and MSI on Sentinel-2A and -2B, with resolutions of 30 and 10–20 m respectively. The development of an harmonised Landsat and Sentinel-2 reflectance product (Claverie et al., 2018) is indeed supporting the synergistic use of these platforms, towards a global mapping of vegetation properties contributing to fire danger at a spatial resolution that is three orders of magnitude higher than operational services, although with longer revisit times as compared to coarser resolution optical sensors.

The study was conducted on a specific study area, for which ad hoc probability distribution functions fitting fire data were identified. The need to determine site-specific statistical models is acknowledged in the scientific literature (Cui and Perera, 2008; Reed and McKelvey, 2002),

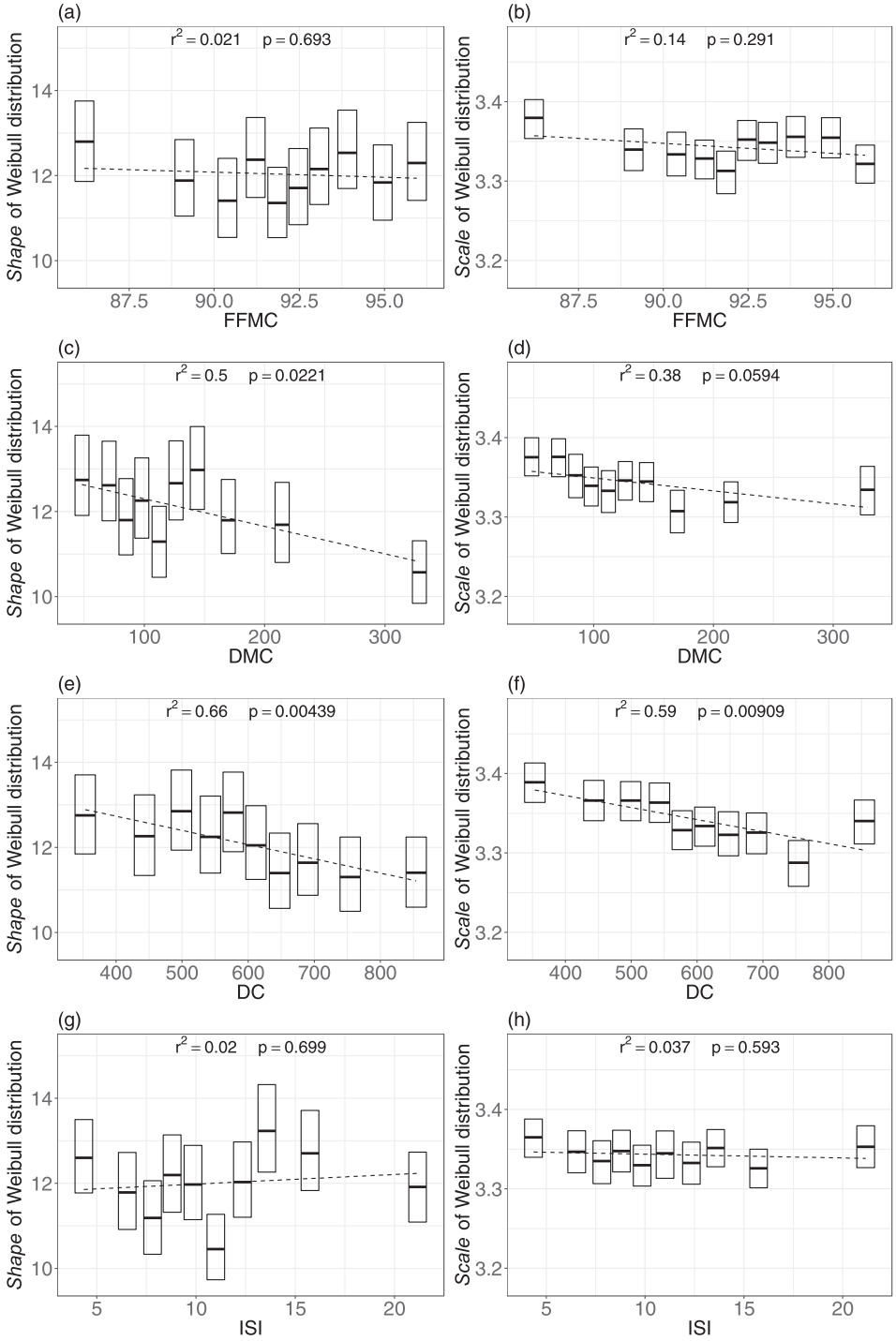

Fig. 11. Plots of shape and scale of Weibull distribution of log-transformed rate of spread, and their 95% confidence intervals, in ten decide bins of the Canadian Forest Fire Weather Index System components: FFMC (a, b), DMC (c, d), DC (e, f), ISI (g, h), BUI (i, j), FWI (k, l). Regression lines refer to the estimated parameters.

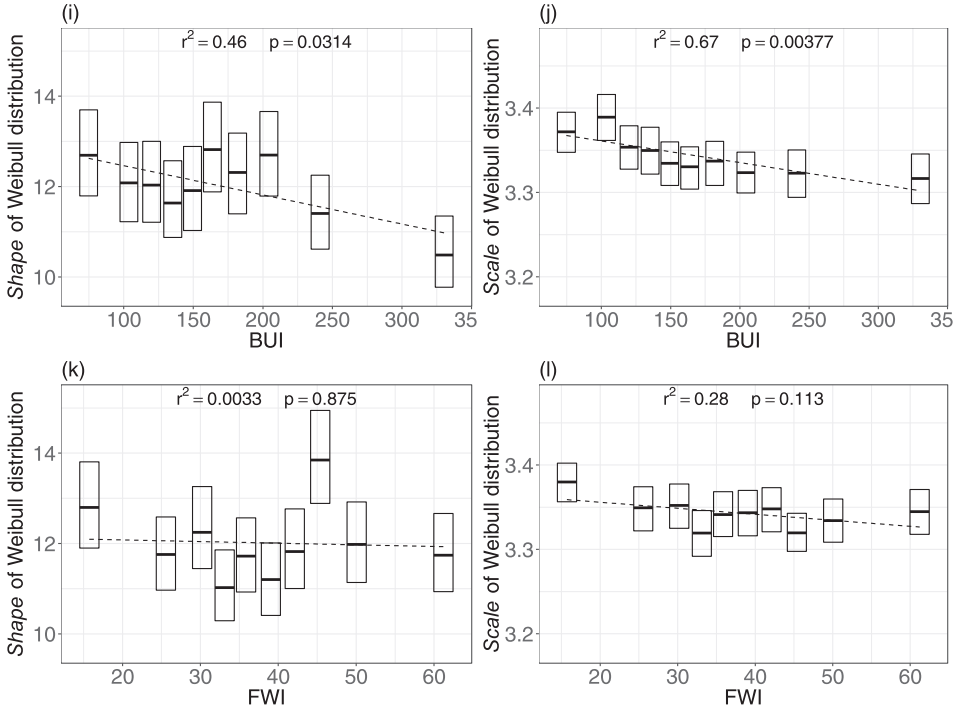

Fig. 11. (*continued*)

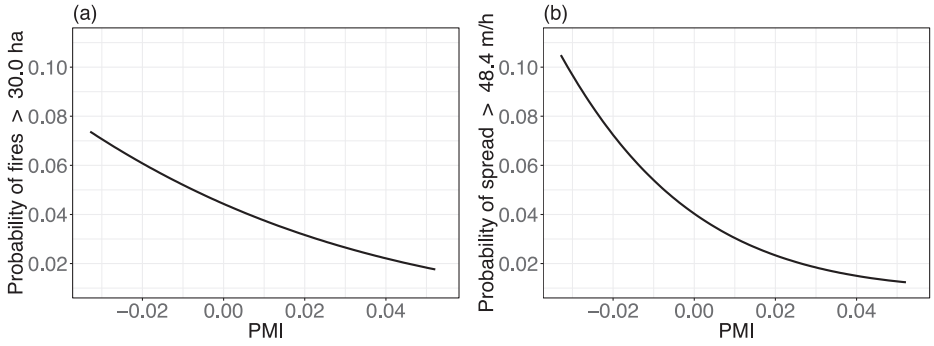

Fig. 12. Modelled probability of extreme events, conditional to ignition, as a function of PMI: probability of fires larger than 30 ha (a); probability of rate of spread higher than 48.6 m/h (b).

suggesting that the applicability of a single global statistical model is unlikely. Nevertheless, the method developed in our study can be implemented elsewhere, as long as similar fire data is available to identify the local probability distribution functions. This is the case of several regional or national fire inventories that are either publicly available on the web, e.g. the Prométhée database in Mediterranean France, the Instituto da Conservação da Natureza e das Florestas (ICNF) fire inventory in Portugal, and the United States Geological Survey (USGS) fire occurrence data in the USA, or are provided upon request by relevant authorities, e.g. the Natural Resources Unit of Carabinieri in Italy and the National Statistical Service in Greece. Such data, along satellite retrievals of PMI, would then serve as a basis for the construction of the local probability distribution functions of burned area and rate of spread conditional to PMI. This in turn would allow the mapping (e.g. daily) of the probability of events exceeding any given threshold, as deemed relevant by fire managers. From an application point of view, fire management and preparedness activities are conducted at regional scales, suggesting that the implementation of regional models for the integration of satellite retrievals in fire danger mapping systems is a viable option.

Declaration of Competing Interest

The authors declare that they have no known competing financial interests or personal relationships that could have appeared to influence the work reported in this paper.

Acknowledgements

This work was supported by the Ministry of Science and Technology of the People's Republic of China (MOST) High Level Foreign Expert program under grant G20190161018. Authors would like to thank Carabinieri (Italian national gendarmerie) and Dipartimento della Protezione Civile (Italian Civil Protection Department) for providing fire data, and Dr. Marc Schleiss for his inspiring observations. We are sincerely grateful to the journal editors and the anonymous reviewers for their insights and constructive comments.

References

Abdollahi, M., Islam, T., Gupta, A., Hassan, Q., 2018. An advanced forest fire danger forecasting system: Integration of remote sensing and historical sources of ignition data. Remote Sens. 10, 923. https://doi.org/10.3390/rs10060923.
Aguado, I., Chuvieco, E., Borén, R., Nieto, H., 2007. Estimation of dead fuel moisture

content from meteorological data in Mediterranean areas. Applications in fire danger assessment. Int. J. Wildl. Fire 16, 390–397. https://doi.org/10.1071/WF06136.
Amato, V., Valletta, M., 2017. Wine landscapes of Italy. In: Soldati, M., Marchetti, M. (Eds.), Landscapes and Landforms of Italy, World Geomorphological Landscapes. Springer International Publishing, Cham, pp. 523–536. https://doi.org/10.1007/978-3-319-26194-2.
Anderson, T.W., Darling, D.A., 1954. A test of goodness of fit. J. Am. Stat. Assoc. 49, 765–769. https://doi.org/10.1080/01621459.1954.10501232.
Andrews, P.L., Cruz, M.G., Rothermel, R.C., 2013. Examination of the wind speed limit function in the Rothermel surface fire spread model. Int. J. Wildl. Fire 22, 959–969. https://doi.org/10.1071/WF12122.
Bajocco, S., Guglietta, D., Ricotta, C., 2015. Modelling fire occurrence at regional scale: does vegetation phenology matter? Eur. J. Remote Sens. 48, 763–775. https://doi.org/10.5721/EuJRS20154842.
Baker, W.L., 1989. Landscape ecology and nature reserve design in the Boundary Waters Canoe Area, Minnesota. Ecology 70, 23–35. https://doi.org/10.2307/1938409.
Barrett, K., Loboda, T., McGuire, A.D., Genet, H., Hoy, E., Kasischke, E., 2016. Static and dynamic controls on fire activity at moderate spatial and temporal scales in the Alaskan boreal forest. Ecosphere 7, e01572. https://doi.org/10.1002/ecs2.1572.
Bianchi, L.O., Defossé, G.E., 2014. Ignition probability of fine dead surface fuels of native Patagonian forests or Argentina. For. Syst. 23, 129–138. https://doi.org/10.5424/fs/2014231-04632.
Bond, W.J., Woodward, F.I., Midgley, G.F., 2005. The global distribution of ecosystems in a world without fire. New Phytol. 165, 525–538. https://doi.org/10.1111/j.1469-8137.2004.01252.x.
Bowyer, P., Danson, F.M., 2004. Sensitivity of spectral reflectance to variation in live fuel moisture content at leaf and canopy level. Remote Sens. Environ. 92, 297–308. https://doi.org/10.1016/j.rse.2004.05.020.
Buitrago Acevedo, M.F., Groen, T.A., Hecker, C.A., Skidmore, A.K., 2017. Identifying leaf traits that signal stress in TIR spectra. ISPRS J. Photogramm. Remote Sens. 125, 132–145. https://doi.org/10.1016/j.isprsjprs.2017.01.014.
Burgan, R.E., 1988. 1988 Revisions to the 1978 National Fire-Danger Rating System. Asheville.
Buitrago Acevedo, M.F., Skidmore, A.K., Groen, T.A., Hecker, C.A., 2018. Connecting infrared spectra with plant traits to identify species. ISPRS J. Photogramm. Remote Sens. 139, 183–200. https://doi.org/10.1016/j.isprsjprs.2018.03.013.
Burgan, R.E., Klaver, R.W., Klaver, J.M., 1998. Fuel models and fire potential from satellite and surface observations. Int. J. Wildl. Fire 8, 159–170. https://doi.org/10.1071/WF9980159.
Cao, X., Cui, X., Yue, M., Chen, J., Tanikawa, H., Ye, Y., 2013. Evaluation of wildfire propagation susceptibility in grasslands using burned areas and multivariate logistic regression. Int. J. Remote Sens. 34, 6679–6700. https://doi.org/10.1080/01431161.2013.805280.
Ceccato, P., Gobron, N., Flasse, S., Pinty, B., Tarantola, S., 2002. Designing a spectral index to estimate vegetation water content from remote sensing data: Part 1 Theoretical approach. Remote Sens. Environ. 82, 188–197. https://doi.org/10.1016/S0034-4257(02)00037-8.
Cheng, T., Rivard, B., Sánchez-Azofeifa, A.G., Féret, J.-B., Jacquemoud, S., Ustin, S.L., 2014. Deriving leaf mass per area (LMA) from foliar reflectance across a variety of plant species using continuous wavelet analysis. ISPRS J. Photogramm. Remote Sens. 87, 28–38. https://doi.org/10.1016/j.isprsjprs.2013.10.009.
Chowdhury, E.H., Hassan, Q.K., 2015. Operational perspective of remote sensing-based forest fire danger forecasting systems. ISPRS J. Photogramm. Remote Sens. 104, 224–236. https://doi.org/10.1016/j.isprsjprs.2014.03.011.
Chuvieco, E., Wagtendonk, J., Riaño, D., Yebra, M., Ustin, S.L., 2009. Estimation of fuel conditions for fire danger assessment. In: Chuvieco, E. (Ed.), Earth Observation of Wildland Fires in Mediterranean Ecosystems. Springer Berlin Heidelberg, Berlin, Heidelberg, pp. 83–96. https://doi.org/10.1007/978-3-642-01754-4_7.
Claverie, M., Ju, J., Masek, J.G., Dungan, J.L., Vermote, E.F., Roger, J.-C., Skakun, S.V., Justice, C., 2018. The Harmonized Landsat and Sentinel-2 surface reflectance data set. Remote Sens. Environ. 219, 145–161. https://doi.org/10.1016/j.rse.2018.09.002.
Corral, Á., Telesca, L., Lasaponara, R., 2008. Scaling and correlations in the dynamics of forest-fire occurrence. Phys. Rev. E 77, 016101. https://doi.org/10.1103/PhysRevE.77.016101.
Cui, W., Perera, A.H., 2008. What do we know about forest fire size distribution, and why is this knowledge useful for forest management? Int. J. Wildl. Fire 17, 234–244. https://doi.org/10.1071/WF06145.
Cumming, S.G., 2001. A parametric model of the fire-size distribution. Can. J. For. Res. 31, 1297–1303. https://doi.org/10.1139/x01-032.
Dasgupta, S., Qu, J.J., 2009. Soil adjusted vegetation water content retrievals in grasslands. Int. J. Remote Sens. 30, 1019–1043. https://doi.org/10.1080/01431160802438548.
Dasgupta, S., Qu, J.J., Hao, X., Bhoi, S., 2007. Evaluating remotely sensed live fuel moisture estimations for fire behavior predictions in Georgia, USA. Remote Sens. Environ. 108, 138–150. https://doi.org/10.1016/j.rse.2006.06.023.
de Groot, W.J., Flannigan, M.D., 2014. Climate change and early warning systems for wildland fire. In: Singh, A., Zommers, Z. (Eds.), Reducing Disaster: Early Warning Systems for Climate Change. Springer Netherlands, Dordrecht, pp. 127–151. https://doi.org/10.1007/978-94-017-8598-3_7.
de Groot, W.J., Wardati, Wang, Y., 2005. Calibrating the Fine Fuel Moisture Code for grass ignition potential in Sumatra. Indonesia. Int. J. Wildl. Fire 14, 161–169. https://doi.org/10.1071/WF04054.
Deeming, J.E., Burgan, R.E., Cohen, J.D., 1977. The National Fire Danger Rating System - 1978. Ogden.
Dimitrakopoulos, A.P., 2001. A statistical classification of Mediterranean species based on their flammability components. Int. J. Wildl. Fire 10, 113–118. https://doi.org/10.1071/WF01004.
Dimitrakopoulos, A.P., Panov, P.I., 2001. Pyric properties of some dominant Mediterranean vegetation species. Int. J. Wildl. Fire 10, 23–27. https://doi.org/10.1071/WF01003.
Dimitrakopoulos, A.P., Papaioannou, K.K., 2001. Flammability assessment of Mediterranean forest fuels. Fire Technol. 37, 143–152. https://doi.org/10.1023/A:1011641601076.
Dowdy, A.J., Mills, G.A., Finkele, K., de Groot, W., 2009. Australian fire weather as represented by the McArthur Forest Fire Danger Index and the Canadian Forest Fire Weather Index. Melbourne.
European Environment Agency, 2007. CLC2006 Technical Guidelines, EEA Technical report. Office for Official Publications of the European Communities, Luxembourg. Doi: 10.2800/12134.
Faivre, N., Jin, Y., Goulden, M.L., Randerson, J.T., 2014. Controls on the spatial pattern of wildfire ignitions in Southern California. Int. J. Wildl. Fire 23, 799–811. https://doi.org/10.1071/WF13136.
Faivre, N.R., Jin, Y., Goulden, M.L., Randerson, J.T., 2016. Spatial patterns and controls on burned area for two contrasting fire regimes in Southern California. Ecosphere 7, e01210. https://doi.org/10.1002/ecs2.1210.
Falk, D.A., Miller, C., McKenzie, D., Black, A.E., 2007. Cross-scale analysis of fire regimes. Ecosystems 10, 809–823. https://doi.org/10.1007/s10021-007-9070-7.
FAO, 2007. Fire Management - Global Assessment 2006.
FAO, 1986. Wildland fire management terminology. Food and Agriculture Organization of the United Nations, Rome.
Feret, J.-B., François, C., Asner, G.P., Gitelson, A.A., Martin, R.E., Bidel, L.P.R., Ustin, S.L., le Maire, G., Jacquemoud, S., 2008. PROSPECT-4 and 5: Advances in the leaf optical properties model separating photosynthetic pigments. Remote Sens. Environ. 112, 3030–3043. https://doi.org/10.1016/j.rse.2008.02.012.
Field, R.D., Spessa, A.C., Aziz, N.A., Camia, A., Cantin, A., Carr, R., de Groot, W.J., Dowdy, A.J., Flannigan, M.D., Manomaiphiboon, K., Pappenberger, F., Tanpipat, V., Wang, X., 2015. Development of a global fire weather database. Nat. Hazards Earth Syst. Sci. 15, 1407–1423. https://doi.org/10.5194/nhess-15-1407-2015.
Finney, M.A., 1998. FARSITE: Fire Area Simulator - Model development and evaluation. Ogden. https://doi.org/10.2737/RMRS-RP-4.
Flannigan, M.D., Wotton, B.M., Marshall, G.A., de Groot, W.J., Johnston, J., Jurko, N., Cantin, A.S., 2016. Fuel moisture sensitivity to temperature and precipitation: climate change implications. Clim. Change 134, 59–71. https://doi.org/10.1007/s10584-015-1521-0.
Fratianni, S., Acquaotta, F., 2017. The climate of Italy. In: Soldati, M., Marchetti, M. (Eds.), Landscapes and Landforms of Italy, World Geomorphological Landscapes. Springer International Publishing, Cham, pp. 29–38. https://doi.org/10.1007/978-3-319-26194-2.
Gao, B.-C., 1996. NDWI - A normalized difference water index for remote sensing of vegetation liquid water from space. Remote Sens. Environ. 58, 257–266. https://doi.org/10.1016/S0034-4257(96)00067-3.
Gao, Y., Walker, J.P., Allahmoradi, M., Monerris, A., Ryu, D., Jackson, T.J., 2015. Optical sensing of vegetation water content: a synthesis study. IEEE J. Sel. Top. Appl. Earth Obs. Remote Sens. 8, 1456–1464. https://doi.org/10.1109/JSTARS.2015.2398034.
Gates, D.M., Keegan, H.J., Schleter, J.C., Weidner, V.R., 1965. Spectral properties of plants. Appl. Opt. 4, 11–20. https://doi.org/10.1364/AO.4.000011.
Gausman, H.W., Allen, W.A., 1973. Optical parameters of leaves of 30 plant species. Plant Physiol. 52, 57–62. https://doi.org/10.1104/pp.52.1.57.
Griffiths, D., 1999. Improved formula for the drought factor in McArthur's forest fire danger meter. Aust. For. 62, 202–206. https://doi.org/10.1080/00049158.1999.10674783.
Haydon, D.T., Friar, J.K., Pianka, E.R., 2000. Fire-driven dynamic mosaics in the Great Victoria Desert, Australia. Landsc. Ecol. 15, 373–381. https://doi.org/10.1023/A:1008138029197.
Hernandez, C., Keribin, C., Drobinski, P., Turquety, S., 2015. Statistical modelling of wildfire size and intensity: a step toward meteorological forecasting of summer extreme fire risk. Ann. Geophys. 33, 1495–1506. https://doi.org/10.5194/angeo-33-1495-2015.
Huesca, M., Litago, J., Merino-de-Miguel, S., Cicuendez-López-Ocaña, V., Palacios-Orueta, A., 2014. Modeling and forecasting MODIS-based Fire Potential Index on a pixel basis using time series models. Int. J. Appl. Earth Obs. Geoinf. 26, 363–376. https://doi.org/10.1016/j.jag.2013.09.003.
Huesca, M., Litago, J., Palacios-Orueta, A., Montes, F., Sebastián-López, A., Escribano, P., 2009. Assessment of forest fire seasonality using MODIS fire potential: a time series approach. Agric. For. Meteorol. 149, 1946–1955. https://doi.org/10.1016/j.agrformet.2009.06.022.
Huete, A.R., 1988. A soil-adjusted vegetation index (SAVI). Remote Sens. Environ. 25, 295–309. https://doi.org/10.1016/0034-4257(88)90106-X.
Hunt, E.R., Rock, B.N., 1989. Detection of changes in leaf water content using near- and middle-infrared reflectances. Remote Sens. Environ. 30, 43–54. https://doi.org/10.1016/0034-4257(89)90046-1.
Jacquemoud, S., Baret, F., 1990. PROSPECT: A model of leaf optical properties spectra. Remote Sens. Environ. 34, 75–91. https://doi.org/10.1016/0034-4257(90)90100-Z.
Jang, J., Viau, A.A., Anctil, F., 2006. Thermal-water stress index from satellite images. Int. J. Remote Sens. 27, 1619–1639. https://doi.org/10.1080/01431160500509194.
Jolly, W.M., Johnson, D.M., 2018. Pyro-ecophysiology: shifting the paradigm of live wildland fuel research. Fire 1, 8. https://doi.org/10.3390/fire1010008.
Keetch, J.J., Byram, G.M., 1968. A Drought Index for Forest Fire Control, U.S.D.A. Forest Service Reseaech Paper SE-38. Asheville, NC.
Lasslop, G., Kloster, S., 2017. Human impact on wildfires varies between regions and with vegetation productivity. Environ. Res. Lett. 12, 115011. https://doi.org/10.1088/

1748-9326/aa8c82.
Leblon, B., 2005. Monitoring forest fire danger with remote sensing. Nat. Hazards 35, 343–359. https://doi.org/10.1007/s11069-004-1796-3.
Leblon, B., Alexander, M., Chen, J., White, S., 2001. Monitoring fire danger of northern boreal forests with NOAA-AVHRR NDVI images. Int. J. Remote Sens. 22, 2839–2846. https://doi.org/10.1080/01431160121183.
Littell, J.S., Peterson, D.L., Riley, K.L., Liu, Y., Luce, C.H., 2016. A review of the relationships between drought and forest fire in the United States. Glob. Chang. Biol. 22, 2353–2369. https://doi.org/10.1111/gcb.13275.
Maffei, C., Alfieri, S.M., Menenti, M., 2018. Relating spatiotemporal patterns of forest fires burned area and duration to diurnal land surface temperature anomalies. Remote Sens. 10, 1777. https://doi.org/10.3390/rs10111777.
Maffei, C., Menenti, M., 2014. A MODIS-based perpendicular moisture index to retrieve leaf moisture content of forest canopies. Int. J. Remote Sens. 35, 1829–1845. https://doi.org/10.1080/01431161.2013.879348.
Maselli, F., 2003. Use of NOAA-AVHRR NDVI images for the estimation of dynamic fire risk in Mediterranean areas. Remote Sens. Environ. 86, 187–197. https://doi.org/10.1016/S0034-4257(03)00099-3.
McArthur, A.G., 1967. Fire Behaviour in Eucalypt Forests. Australia Forestry and Timber Bureau, Canberra.
Menenti, M., Malamiri, H.R.G., Shang, H., Alfieri, S.M., Maffei, C., Jia, L., 2016. Observing the response of terrestrial vegetation to climate variability across a range of time scales by time series analysis of land surface temperature. In: Ban, Y. (Ed.), Multitemporal Remote Sensing. Springer International Publishing, Cham, pp. 277–315. Doi: 10.1007/978-3-319-47037-5_14.
Modugno, S., Balzter, H., Cole, B., Borrelli, P., 2016. Mapping regional patterns of large forest fires in Wildland-Urban Interface areas in Europe. J. Environ. Manage. 172, 112–126. https://doi.org/10.1016/j.jenvman.2016.02.013.
Molod, A., Takacs, L., Suarez, M., Bacmeister, J., 2015. Development of the GEOS-5 atmospheric general circulation model: evolution from MERRA to MERRA2. Geosci. Model Dev. 8, 1339–1356. https://doi.org/10.5194/gmd-8-1339-2015.
Montagné-Huck, C., Brunette, M., 2018. Economic analysis of natural forest disturbances: A century of research. J. For. Econ. 32, 42–71. https://doi.org/10.1016/j.jfe.2018.03.002.
Moritz, M.A., 1997. Analyzing Extreme disturbance events: Fire in Los Padres National Forest. Ecol. Appl. 7, 1252–1262. https://doi.org/10.2307/2641212.
Mousivand, A., Menenti, M., Gorte, B., Verhoef, W., 2014. Global sensitivity analysis of the spectral radiance of a soil–vegetation system. Remote Sens. Environ. 145, 131–144. https://doi.org/10.1016/j.rse.2014.01.023.
Nolan, R.H., Boer, M.M., Resco de Dios, V., Caccamo, G., Bradstock, R.A., 2016. Large-scale, dynamic transformations in fuel moisture drive wildfire activity across southeastern Australia. Geophys. Res. Lett. 43, 4229–4238. https://doi.org/10.1002/2016GL068614.
Nolan, R.H., Hedo, J., Arteaga, C., Sugai, T., Resco de Dios, V., 2018. Physiological drought responses improve predictions of live fuel moisture dynamics in a Mediterranean forest. Agric. For. Meteorol. 263, 417–427. https://doi.org/10.1016/j.agrformet.2018.09.011.
Pan, J., Wang, W., Li, J., 2016. Building probabilistic models of fire occurrence and fire risk zoning using logistic regression in Shanxi Province. China. Nat. Hazards 81, 1879–1899. https://doi.org/10.1007/s11069-016-2160-0.
Pausas, J.G., Ribeiro, E., 2013. The global fire-productivity relationship. Glob. Ecol. Biogeogr. 22, 728–736. https://doi.org/10.1111/geb.12043.
Pellegrini, A.F.A., Ahlström, A., Hobbie, S.E., Reich, P.B., Nieradzik, L.P., Staver, A.C., Scharenbroch, B.C., Jumpponen, A., Anderegg, W.R.L., Randerson, J.T., Jackson, R.B., 2018. Fire frequency drives decadal changes in soil carbon and nitrogen and ecosystem productivity. Nature 553, 194–198. https://doi.org/10.1038/nature24668.
Pellizzaro, G., Cesaraccio, C., Duce, P., Ventura, A., Zara, P., 2007a. Relationships between seasonal patterns of live fuel moisture and meteorological drought indices for Mediterranean shrubland species. Int. J. Wildl. Fire 16, 232–241. https://doi.org/10.1071/WF06081.
Pellizzaro, G., Duce, P., Ventura, A., Zara, P., 2007b. Seasonal variations of live moisture content and ignitability in shrubs of the Mediterranean Basin. Int. J. Wildl. Fire 16, 633–641. https://doi.org/10.1071/WF05088.
Pimont, F., Ruffault, J., Martin-StPaul, N.K., Dupuy, J.-L., 2019. Why is the effect of live fuel moisture content on fire rate of spread underestimated in field experiments in shrublands? Int. J. Wildl. Fire 28, 127–137. https://doi.org/10.1071/WF18091.
Podschwit, H.R., Larkin, N.K., Steel, E.A., Cullen, A., Alvarado, E., 2018. Multi-model forecasts of very-large fire occurences during the end of the 21st century. Climate 6, 100. https://doi.org/10.3390/cli6040100.
Preisler, H.K., Brillinger, D.R., Burgan, R.E., Benoit, J.W., 2004. Probability based models for estimation of wildfire risk. Int. J. Wildl. Fire 13, 133–142. https://doi.org/10.1071/WF02061.
Preisler, H.K., Burgan, R.E., Eidenshink, J.C., Klaver, J.M., Klaver, R.W., 2009. Forecasting distributions of large federal-lands fires utilizing satellite and gridded weather information. Int. J. Wildl. Fire 18, 508. https://doi.org/10.1071/WF08032.
Pyne, S.J., Andrews, P.L., Laven, R.D., 1996. Introduction to Wildland Fire, 2nd ed. John Wiley & Sons Inc, New York.
Quan, X., He, B., Li, X., Tang, Z., 2015. Estimation of grassland live fuel moisture content from ratio of canopy water content and foliage dry biomass. IEEE Geosci. Remote Sens. Lett. 12, 1903–1907. https://doi.org/10.1109/LGRS.2015.2437391.
Reed, W.J., McKelvey, K.S., 2002. Power-law behaviour and parametric models for the size-distribution of forest fires. Ecol. Modell. 150, 239–254. https://doi.org/10.1016/S0304-3800(01)00483-5.
Riaño, D., Vaughan, P., Chuvieco, E., Zarco-Tejada, P.J., Ustin, S.L., 2005. Estimation of fuel moisture content by inversion of radiative transfer models to simulate equivalent water thickness and dry matter content: Analysis at leaf and canopy level. IEEE Trans. Geosci. Remote Sens. 43, 819–826. https://doi.org/10.1109/TGRS.2005.843316.
Rossa, C.G., Fernandes, P.M., 2017. On the effect of live fuel moisture content on fire-spread rate. For. Syst. 26, eSC08. https://doi.org/10.5424/fs/2017263-12019.
Rossa, C.G., Veloso, R., Fernandes, P.M., 2016. A laboratory-based quantification of the effect of live fuel moisture content on fire spread rate. Int. J. Wildl. Fire 25, 569–573. https://doi.org/10.1071/WF15114.
Rothermel, R.C., 1991. Predicting behavior and size of crown fires in the northern Rocky Mountains. Ogden. https://doi.org/10.2737/INT-RP-438.
Rothermel, R.C., 1972. A mathematical model to predicting fire spread in wildland fuels.
Ruffault, J., Martin-StPaul, N., Pimont, F., Dupuy, J.-L., 2018. How well do meteorological drought indices predict live fuel moisture content (LFMC)? An assessment for wildfire research and operations in Mediterranean ecosystems. Agric. For. Meteorol. 262, 391–401. https://doi.org/10.1016/j.agrformet.2018.07.031.
San-Miguel-Ayanz, J., Durrant, T., Boca, R., Libertà, G., Branco, A., de Rigo, D., Ferrari, D., Maianti, P., Artés Vivancos, T., Costa, H., Lana, F., Löffler, P., Nuijten, D., Ahlgren, A.C., Leray, T., 2018. Forest Fires in Europe, Middle East and North Africa 2017. Luxembourg. https://doi.org/10.2760/663443.
San-Miguel-Ayanz, J., Schulte, E., Schmuck, G., Camia, A., Strobl, P., Liberta, G., Giovando, C., Boca, R., Sedano, F., Kempeneers, P., McInerney, D., Withmore, C., de Oliveira, S.S., Rodrigues, M., Durrant, T., Corti, P., Oehler, F., Vilar, L., Amatulli, G., 2012. Comprehensive Monitoring of Wildfires in Europe: The European Forest Fire Information System (EFFIS). In: Tiefenbacher, J. (Ed.), Approaches to Managing Disaster - Assessing Hazards, Emergencies and Disaster Impacts. InTech, Rijeka, pp. 87–108. Doi: 10.5772/28441.
Seidl, R., Thom, D., Kautz, M., Martin-Benito, D., Peltoniemi, M., Vacchiano, G., Wild, J., Ascoli, D., Petr, M., Honkaniemi, J., Lexer, M.J., Trotsiuk, V., Mairota, P., Svoboda, M., Fabrika, M., Nagel, T.A., Reyer, C.P.O., 2017. Forest disturbances under climate change. Nat. Clim. Chang. 7, 395–402. https://doi.org/10.1038/nclimate3303.
Stow, D., Niphadkar, M., Kaiser, J., 2006. Time series of chaparral live fuel moisture maps derived from MODIS satellite data. Int. J. Wildl. Fire 15, 347–360. https://doi.org/10.1071/WF05060.
Syphard, A.D., Sheehan, T., Rustigian-Romsos, H., Ferschweiler, K., 2018. Mapping future fire probability under climate change: Does vegetation matter? PLoS One 13, e0201680. https://doi.org/10.1371/journal.pone.0201680.
Taylor, S.W., Alexander, M.E., 2006. Science, technology, and human factors in fire danger rating: the Canadian experience. Int. J. Wildl. Fire 15, 121–135. https://doi.org/10.1071/WF05021.
Tucker, C.J., 1980. Remote sensing of leaf water content in the near infrared. Remote Sens. Environ. 10, 23–32. https://doi.org/10.1016/0034-4257(80)90096-6.
Ullah, S., Skidmore, A.K., Ramoelo, A., Groen, T.A., Naeem, M., Ali, A., 2014. Retrieval of leaf water content spanning the visible to thermal infrared spectra. ISPRS J. Photogramm. Remote Sens. 93, 56–64. https://doi.org/10.1016/j.isprsjprs.2014.04.005.
Ustin, S.L., Riaño, D., Koltunov, A., Roberts, D.A., Dennison, P.E., 2009. Mapping fire risk in Mediterranean ecosystems of California: vegetation type, density, invasive species, and fire frequency. In: Earth Observation of Wildland Fires in Mediterranean Ecosystems. Springer Berlin Heidelberg, Berlin, Heidelberg, pp. 41–53. Doi: 10.1007/978-3-642-01754-4_4.
Van Wagner, C.E., 1987. Development and structure of the Canadian Fire Weather Index System. Ottawa.
Vermote, E.F., El Saleous, N., Justice, C.O., Kaufman, Y.J., Privette, J.L., Remer, L., Roger, J.C., Tanré, D., 1997. Atmospheric correction of visible to middle-infrared EOS-MODIS data over land surfaces: background, operational algorithm and validation. J. Geophys. Res. Atmos. 102, 17131–17141. https://doi.org/10.1029/97JD00201.
Vermote, E.F., Roger, J.C., Ray, J.P., 2015. MODIS surface reflectance user's guide - Collection 6.
Vermote, E.F., Vermeulen, A., 1999. MODIS ATBD - Atmospheric correction algorithm: spectral reflectances (MOD09).
Verrelst, J., Camps-Valls, G., Muñoz-Marí, J., Rivera, J.P., Veroustraete, F., Clevers, J.G.P.W., Moreno, J., 2015. Optical remote sensing and the retrieval of terrestrial vegetation bio-geophysical properties – A review. ISPRS J. Photogramm. Remote Sens. 108, 273–290. https://doi.org/10.1016/j.isprsjprs.2015.05.005.
Verstraete, M.M., Pinty, B., 1996. Designing optimal spectral indexes for remote sensing applications. IEEE Trans. Geosci. Remote Sens. 34, 1254–1265. https://doi.org/10.1109/36.536541.
Vicente-Serrano, S.M., Gouveia, C., Camarero, J.J., Beguería, S., Trigo, R., López-Moreno, J.I., Azorín-Molina, C., Pasho, E., Lorenzo-Lacruz, J., Revuelto, J., Morán-Tejeda, E., Sanchez-Lorenzo, A., 2013. Response of vegetation to drought time-scales across global land biomes. Proc. Natl. Acad. Sci. 110, 52–57. https://doi.org/10.1073/pnas.1207068110.
Viegas, D.X., Viegas, M.T., 1994. A relationship between rainfall and burned area for portugal. Int. J. Wildl. Fire 4, 11–16. https://doi.org/10.1071/WF9940011.
Weber, M.G., Stocks, B.J., 1998. Forest fires in the boreal forests of Canada. In: Moreno, J.M. (Ed.), Large Forest Fires. Backhuys Publishers, Leiden, pp. 215–233.
Williams, A.P., Abatzoglou, J.T., 2016. Recent advances and remaining uncertainties in resolving past and future climate effects on global fire activity. Curr. Clim. Change Reports 2, 1–14. https://doi.org/10.1007/s40641-016-0031-0.
Wolfe, R.E., Nishihama, M., Fleig, A.J., Kuyper, J.A., Roy, D.P., Storey, J.C., Patt, F.S., 2002. Achieving sub-pixel geolocation accuracy in support of MODIS land science.

Remote Sens. Environ. 83, 31–49. https://doi.org/10.1016/S0034-4257(02)00085-8.
Woolley, J.T., 1971. Reflectance and transmittance of light by leaves. Plant Physiol. 47, 656–662. https://doi.org/10.1104/pp.47.5.656.
Yebra, M., Chuvieco, E., 2009. Generation of a species-specific look-up table for fuel moisture content assessment. IEEE J Sel. Top. Appl. Earth Obs. Remote Sens. 2, 21–26. https://doi.org/10.1109/JSTARS.2009.2014008.
Yebra, M., Dennison, P.E., Chuvieco, E., Riaño, D., Zylstra, P., Hunt, E.R., Danson, F.M., Qi, Y., Jurdao, S., 2013. A global review of remote sensing of live fuel moisture content for fire danger assessment: Moving towards operational products. Remote Sens. Environ. 136, 455–468. https://doi.org/10.1016/j.rse.2013.05.029.
Yebra, M., Quan, X., Riaño, D., Rozas Larraondo, P., van Dijk, A.I.J.M., Cary, G.J., 2018. A fuel moisture content and flammability monitoring methodology for continental Australia based on optical remote sensing. Remote Sens. Environ. 212, 260–272. https://doi.org/10.1016/j.rse.2018.04.053.
Zarco-Tejada, P.J., Rueda, C.A., Ustin, S.L., 2003. Water content estimation in vegetation with MODIS reflectance data and model inversion methods. Remote Sens. Environ. 85, 109–124. https://doi.org/10.1016/S0034-4257(02)00197-9.